國立臺灣大學獸醫專業學院獸醫所基礎組

碩士論文

Graduate Institute of Veterinary Medicine
School of Veterinary Medicine
National Taiwan University

Master Thesis

探討副睪中第一型硫氫氧化酶的分泌調控機制

Investigation of the Regulatory Mechanism of Epididymal Quiescin Q6 Sulfhydryl Oxidase 1 Protein Secretion

林宛臻

Wan-Zhen Lin

指導教授：蔡沛學 博士

Advisor: Pei-Shiue Tsai, Ph.D.

中華民國 108 年 8 月

August 2019

doi:10.6342/NTU201903813

致謝

很榮幸兩年前能加入 JT Lab 這個大家庭，讓我這個從 0 開始的研究生可以在愛與包容的幸福環境中成長，兩年前的自己完全沒有想到可以完成一本論文，也沒有想到兩年的收穫可以這麼多，不僅是學識上的進步，我比以前更有自信的面對困境並學會自己解決問題的能力，也更懂得思辯應答的技巧。

這一路上遇到的人都是貴人，首先最感謝的是蔡老師，總是把學生當女兒在關心，不只照顧我們的五臟六腑，也教導了很多做人處事的道理，最崇拜老師解說的能力，可以用有趣的方式敘述自己的研究，並且成功吸引大家的注意力，另外，老師也是給我們最多包容和耐心的人，總是用“learning process”來降低我們實驗失敗的罪惡感，讓我們可以大膽的試驗自己的想法，也有更多獨立思考的空間。再來也謝謝實驗室的學姊 Joan，Radhika 和 Betty，能在我徬徨的時候拉我一把，給我許多身心靈的支持與幫助，很開心能認識來自印度的 Radhika，讓生活更國際化外也讓我的英文口說更流利。謝謝 Betty 總是用溫暖的擁抱鼓勵我。其中尤其感謝同一個實驗計畫的 Joan 學姊，很有耐心地從基礎教我，也讓我了解腦袋思考的東西才是最重要的，如何有效的思考問題、解決問題才是無法被取代的技能。也謝謝同屆的朋友們: 佳蓉、信慈、淳媛，在實驗做不出來的時候互相鼓勵或報完 seminar 後一起唱歌放鬆，在碩士生涯的路上有大家互相扶持進步，讓碩士生活精彩豐富。

最後感謝生活中最親密的家人和宥任，在我受挫折時可以有一個避風港，永遠對我張開最溫暖的懷抱聆聽我的煩惱、在我實驗順利時一同分享我的喜悅也支持著我的任何決定，結束最後的學生身分後，接下來我會帶著在研究所所學回饋給社會，希望能在生醫領域有更多有用的貢獻。

doi:10.6342/NTU201903813

中文摘要

哺乳類動物的精子經由睪丸製造釋出後尚未完全成熟，精子要在副睪中進行不同形式與程度的蛋白質轉譯後修飾才會獲得完整的受孕能力與活動力，眾多修飾過程中，雙硫鍵催化過程對於精子的蛋白質結構穩定和頭部染色體濃縮扮演著很重要的角色。過去我們實驗室之前透過蛋白質鑑定，找到了一個參與雙硫鍵催化過程的關鍵蛋白質: 第一型精漿蛋白硫氫氧化（quiescin sulfhydryl oxidase 1, QSOX1），並且發現此蛋白質在副睪的不同區段 (前、中、後) 有不同的含量，此外，也發現此蛋白質可附著於副睪前端精子的頂體區域，然而此蛋白質在精子成熟過程中扮演的角色尚未被完全瞭解。

本論文希望藉由探討 QSOX1 的分泌調控機制，讓我們更加了解此蛋白在副睪中的特性，進而在未來能進一步探討 QSOX1 在精子成熟過程中的所扮演的角色。透過西方墨點法及免疫螢光染色法，我們發現 QSOX1 的分泌在 30 天大的小鼠副睪中有顯著的上升， 此結果說明調控此蛋白質分泌的機制可能是透過體內睪固酮的增加或是透過副睪管腔中精子的刺激而導致，藉由二維共培養系統的建立，我們進一步測試上述兩個者對 QSOX1 的分泌是否具有影響，結果顯示，加入睪固酮對於QSOX1的分泌並沒有顯著的影響，而在精子共培養的組別中，培養液中的QSOX1有顯著性的增加。此外，相較於副睪後段較成熟的精子，副睪前端的精子能更有效的刺激 QSOX1 的分泌。透過高效液相層析串聯質譜儀分析和比較蛋白質體分析，我們進一步從培養液中鑑定出額外的 582 個分泌型蛋白質，推測其中的一些 （258 個）蛋白質可能由精子釋放並刺激 QSOX1 的分泌。

綜合以上結果，QSOX1 的分泌主要是經由精子的刺激而不是由睪固酮，但其作用分子與機制與切確的刺激因子為何有待進一步的研究。

關鍵詞: 副睪蛋白質分泌，精漿蛋白硫氫氧化酶 1，精子共培養系統，蛋白質體學分析

doi:10.6342/NTU201903813

Abstract

Spermatozoa are not fully mature after being released from the testis. They gradually become mature and acquire the capacity for progressive motility and fertilization ability through post-translational modifications that occur in different segments of the epididymis. Among these modifications, disulfide bond formation is essential for sperm protein and structure stability, including chromatin condensation, sperm midpiece, and tail stabilization. The quiescin sulfhydryl oxidase 1 (QSOX1), which catalyzes the thiol-oxidation reaction has been identified in the epididymis. We have demonstrated that QSOX1 exhibits a region-specific distribution in the epididymis, and appears at the acrosome region of the caput sperm. However, the functional role and the regulation of QSOX1 secretion in the epididymis are still unknown.

This thesis focuses on the understanding of secretory regulation of QSOX1 in the epididymis. Through Western blotting and indirect immunofluorescent studies, we showed that mouse secretory QSOX1 was upregulated at postnatal day 30, suggesting the potential involvement of testosterone and/or sperm cells on the regulation and stimulation of QSOX1 secretion. To closely mimic *in vivo* situation, we set up a 2D polarized co-culture system to investigate the effects of these stimuli and to measure the level of QSOX1 secretion *in vitro*. Our data showed that QSOX1 secretion was increased after

doi:10.6342/NTU201903813

co-incubating with sperm cells (especially in caput sperm cells) but not when co-incubating with testosterone or its metabolites, DHT. Liquid chromatography-tandem mass spectrometry (LC-MS/MS) and comparing proteome analysis were used to identify and characterize the possible regulatory molecules that were being released from sperm. We identified 582 secretory proteins that were exclusively present in the sperm-enriched group and further categorized 258 caput sperm proteins that might be responsible for stimulating QSOX1 secretion in the epididymis.

In conclusion, our study provides solid evidence that QSOX1 secretion is likely regulated by sperm-epididymis epithelium interaction rather than by testosterone stimulation. This result may further explain the role of QSOX1 upon sperm maturation.

Key words: epididymal protein secretion, QSOX1, sperm co-culture, proteome analysis

doi:10.6342/NTU201903813

Content

doi:10.6342/NTU201903813

doi:10.6342/NTU201903813

doi:10.6342/NTU201903813

List of Figures

doi:10.6342/NTU201903813

doi:10.6342/NTU201903813

List of Tables

doi:10.6342/NTU201903813

CHAPTER1 Introduction

1.1. Interactions between spermatozoa and the epididymis

Produced by the testis, mammalian spermatozoa completed their morphological changes (i.e. spermiogenesis) within the testis. They gain additional fertility and motility after undergoing post-testicular modifications in the epididymis. The idea of post-testicular modification was first described in the early nineteenth century, and later been proven to be essential for spermatozoa maturation and storage [1-3].

The epididymis is a long, complex, convoluted duct with a single layer of epithelium surrounding the lumen and connects the efferent ducts to the vas deferens [4]. The composition of epididymal epithelial cells contain several cell types creating a complex microenvironment suitable for the maturating spermatozoa, Anatomically, the epididymis consists of three main regions, from head to tail are caput, corpus, and cauda. Each region exhibits a highly regional-specific microenvironment because the proportion of different cell types sequentially changes throughout the epididymis [5, 6]. In addition, the epididymal-blood barrier restricts the exchange between luminal components and blood plasma and thus protect spermatozoa from circulating toxic components during their last maturation steps [7].

doi:10.6342/NTU201903813

Due to the characteristics described above, spermatozoa progressively change their maturation status in parallel with the changes of the epididymal microenvironment, indicates that epididymis plays an important and essential role in spermatozoa maturation, transport, concentrate, protection, and storage [8]. During this sequential modification, spermatozoa lack active gene transcription and *de novo* protein translation [9]; therefore, all those additional changes on sperm were primarily driven by interactions between spermatozoa and the complex components bathed within the epididymal lumen and lead to protein, sugar, lipid additional to or removal from the sperm membrane surface [10].

1.2. **The importance of disulfide bond formation during sperm transit in the epididymis**

During post-testicular modification processes, spermatozoa undergo substantial remodeling on the membrane. The changes of sperm membrane composition could result from the removal of surface proteins from the testicular sperm, modifications on the pre-existing surface proteins or the binding of additional epididymal proteins to the maturing epididymal spermatozoa [6]. Among different changes and modifications, the disulfide bond formation process is essential for the stabilization of sperm structure. Disulfide bonds are formed between the sulfur atoms of pairs of cysteine residues

doi:10.6342/NTU201903813

within or across proteins and can affect protein structure and/or functions. Studies have suggested that oxidation of thiol groups can stabilize various sperm structures, including chromatin, sperm midpiece and tail (Fig. 1) [11].

1.2.1. Membrane modification

The amount of disulfide bond on the sperm membrane (in both head and tail) exhibits a progressive increase from caput toward cauda epididymis and coincides with the advances of maturation stages of sperm cells, the evidence supporting that disulfide bond formation on the spermatozoa is a part of the maturation process during sperm epididymal transit [12]. Among different maturation processes, the increased potential for forwarding motility is the most obvious alteration [13]. Scientists had demonstrated that sulfhydryl oxidation is important for the maintenance and stabilization of sperm tail structure and contributes to normal motility wave patterns [14, 15]. During epididymal transit, the beating pattern of sperm flagellar gradually becomes more vigorous [16]. Many proteins have been shown to be sperm motility-promoting proteins after additional disulfide bonds were formed within their protein structure. For example, outer dense fiber protein 1 (ODF1), one of the flagellar proteins are oxidized to form disulfides during epididymal transit and is associated with the bending torque of the tail.

doi:10.6342/NTU201903813

Hetherington et al. demonstrated that sperm cells from OFD1 knock out mice exhibit thinner filament fibers and fail to fertilize oocyte [17].

1.2.2. Nucleus stabilization

It has been reported that sperm chromatin condensation was positively correlated to sperm capacity for fertilizing an oocyte in natural [18]. Disulfide bond formation occurs within sperm nuclear protamine is part of sperm chromatin condensation processes [19]. Much of the research showed that protamine can condense sperm chromatin and stabilized the sperm head morphology by forming the intermolecular disulfide bonds to sperm DNA [20]. Condensation of sperm chromatin is essential for fertility, and early embryo development, therefore, intermolecular disulfide bonds formation is required for the acquisition of fertilization ability of spermatozoa [21].

Base on the above-mentioned studies, disulfide bond formation plays a critical role during sperm maturation. Defects in disulfide bond formation will result in sperm dysfunction and fertility failure. However, the exact mechanism of thiol to disulfide bond processes as well as candidate proteins trigger or regulate this fertility essential process in the epididymis is still unclear.

doi:10.6342/NTU201903813

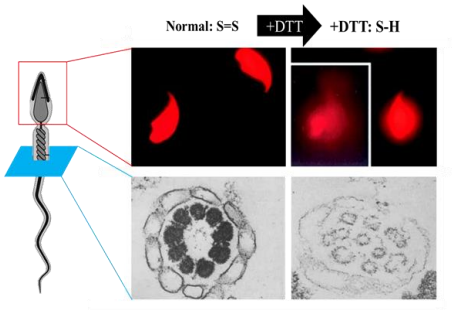

A. Condense sperm chromatin

B. Stabilize mitochondria membrane and fiber

Figure 1. Importance of disulfide bond formation to sperm stabilization.

(modified from [22, 23])

1.3. **Introduction of QSOX1 protein**

The quiescin sulfhydryl oxidase (QSOX), which can catalyze the thiol-oxidation reaction 2R-SH + O_2 → R-SS-R + H_2O_2, have been identified in several tissues including in male genital tract in mammalian species [24]. The possible functions of QSOX protein in the male genital tract were first described in the epididymal and seminal fluids of rodent species [25]. These include generation of disulfide bonds within seminal plasma proteins or spermatozoa, the preservation of spermatozoan membrane integrity, antimicrobial activity (through the release of H_2O_2), and the protection of spermatozoa against the harmful effects of thiol after ejaculation [26].

There are two known isoforms of QSOX proteins, QSOX1 and QSOX2, and in this thesis, we focus specifically on QSOX1 isoform. *QSOX1* was observed up-regulated in human fibroblasts when these cells reached quiescence state, hence being named the Quiescin Q6 gene at first discovery [27]. QSOX1 protein is characterized as

doi:10.6342/NTU201903813

a FAD-dependent transmembrane protein with two functional domains: the N-terminal thioredoxin TRX domain which can catalyze disulfide bond formation, and the C-terminal Erv enzyme domain which is responsible for redox reaction [28]. QSOX1 is ubiquitously expressed in almost all organs/tissues, and its expression level is particularly high in the tissue involved in disulfide-rich proteins secretion (for example skin apocrine glands, pancreas, reproductive tracts), suggesting QSOX1 may involve in the oxidative folding process of secreted proteins [24, 29, 30]. At the cellular level, QSOX1 protein can be detected in the ER, Golgi and secretory granules indicating QSOX1 may participate in disulfide bond formation of secretory proteins that are regulated by secretory pathway [29, 31, 32]. In addition to protein folding, QSOX1 has also been shown to involve in the elaboration of the extracellular matrix, redox regulation, cell cycle control [27, 30, 33].

1.3.1. QSOX1 variants

Two splice variants of the human *QSOX1* gene have been reported, QSOX1a with a complete transmembrane domain is translated by the whole sequence of 3314 nucleotide bases, which encodes 747 amino acids. QSOX1b, a spliced variant from QSOX1a, is a secretory protein in the absence of the transmembrane domain, which encodes a peptide of 604 amino acids [27, 29]. Based on their cellular localization and

doi:10.6342/NTU201903813

properties, QSOX1a may trigger the disulfide bonds formation within the cell or on the cell surface, whereas QSOX1b may function as a secreted oxidase to inhibit the function of extracellular reducing agents [34].

1.3.2. QSOX1 in the epididymis and its relationship with sperm

In the epididymis, QSOX1 is detected mainly in the principal cells. The secretory QSOX1 isoform in mouse is called QSOX1c with a molecular weight of 63kDa, it is the dominant isoform detected in the mouse epididymis, and shows region-specific distribution through the epididymis. From the immunofluorescence staining of our earlier study, QSOX1c is first detected in the distal region of the caput epididymis and progressively enrich from caput toward cauda (Fig. 2). The luminal detection of QSOX1c suggests that this protein may be secreted into the lumen by epididymal epithelial cells and likely play a role at different maturating stages of spermatozoa [35].

The activity of sulfhydryl oxidase in the epididymis has been described by Chang and Morton in 1975, and this activity can maintain thiol/disulfide homeostasis of sperm cells without any additional need of cofactors. They suggested that this protein is a protective enzyme that can preserve spermatozoa structure and function in the epididymis [36]. From our earlier data, we observed that QSOX1c associated at different regions of sperm surface on the sperm head, mid-piece, and principal piece of

doi:10.6342/NTU201903813

the tail (Fig. 3) [35]. However, the regulatory pathway directing QSOX1c secretion and the actual functions of the QSOX1c association on the sperm membrane surface and its relationship with the sperm maturation process remain unknown.

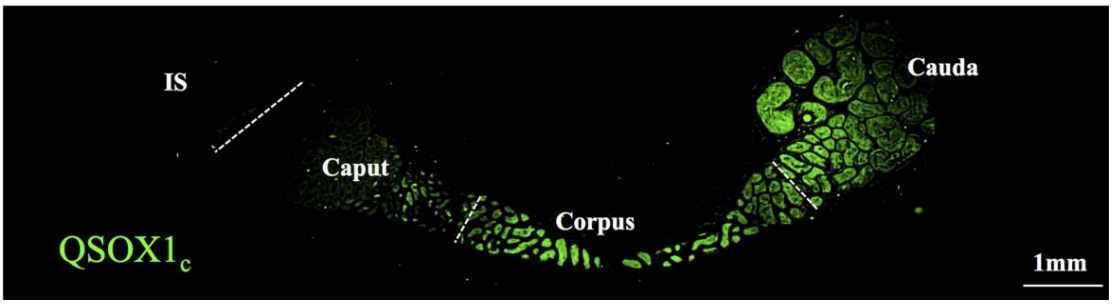

Figure 2. QSOX1c shows the region-specific distribution in the mouse epididymis. [35]

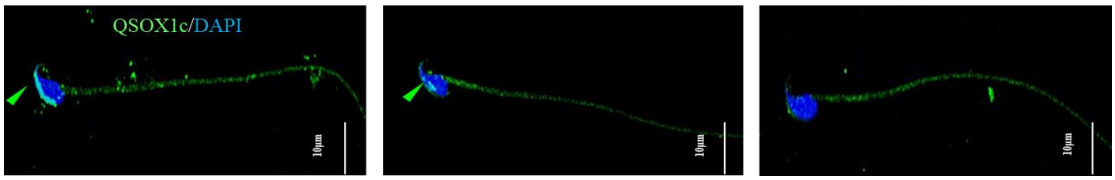

Figure 3. QSOX1c exhibits distinctive association on different maturation status sperm. [35]

doi:10.6342/NTU201903813

1.4. **Protein secretion in the epididymis**

1.4.1. Different secretory pathways

The proteins in the epididymal lumen are originating from various sources [6]. (1) Testicular compounds flow into the proximal region of the epididymis through the efferent ducts: these components, for instance, testicular factor basic fibroblast growth factor can regulate gamma-glutamyl transpeptidase activity in the epididymis can normally be rapidly absorbed by the caput region of the epididymis. [37]. (2) The *de novo* proteins synthesized and secreted by epididymis epithelial cells: for example, WAP-type four-disulfide core domain protein 8 (WFDC8) [38]. (3) Proteolysis products from the pre-existing proteins within the original luminal environment: for example, angiotensin I-converting enzyme (ACE) which is known as a proteolysis product of sperm protein [39]. (4) Metabolic byproducts originated from spermatozoa during the transition and maturation processes. For instance, acetylcarnitine is a byproduct of sperm energy metabolism [40].

Among all the above-mentioned protein sources, proteins that are synthesized and secreted by epididymal epithelium cells contribute to the major protein source found in the epididymis lumen [6]. The protein secretory activity can be divided into two major pathways, the classical merocrine secretion, and the non-classical apocrine secretion.

doi:10.6342/NTU201903813

In the classical pathway of merocrine secretion, the principal cells featured protein secretion contain abundant rough endoplasmic reticulum (ER), a large Golgi complex and detectable coated pits on the apical side of the cell surface [41, 42]. Proteins that are classified into this secretory pathway are synthesized in the ER, glycosylated in the Golgi complex, and then packed into large secretory granules (150-300 nm) or small Golgi derived vesicles (60-70 nm) [43]. Those vesicles contain proteins formed by the Golgi will subsequently move to and fuse with the cell surface plasma membrane and then release those contents into the epididymal lumen [44-46]. Some researches indicated that the secretion activity of large secretory granules are mostly regulated by specific stimuli, while the small vesicles undergo the constitutive secretion without any additional stimulation [47].

Another secretory pathway called apocrine secretion is ER/Golgi independent non-classical pathway. It has been reported that the biosynthesis of proteins that will undergo apocrine secretion is hormone-dependent [48]. Membrane-bound secretory granules are not involving in this pathway, rather, a portion of the plasma membrane from the apical cell shows the protrusions blebs upon the release of vesicle contents. In the epididymal principal cells, these blebs are directed towards the lumen side [49]. Although scientists initially considered those apical bleb structures were artifacts from fixation procedures during electron microscopy staining, but later advanced fixation

doi:10.6342/NTU201903813

methods proved the vascular perfusion and apical blebs are prominent features of principal cells in several species [50, 51]. In the mouse and human epididymis, apical blebs are observed throughout the entire lumen and exhibit different morphologies, suggesting that the formation process is dynamic and heterogeneous. After apical blebs detach from the membrane surface and release into the lumen, the membrane of these blebs become fragmented and their contents including ER elements, free ribosomes, glycogen and vesicle of various sizes, such as epididymosome can thereafter be released.

1.4.2. Potential regulation mechanisms for epididymal protein secretion

Previous studies have reported that half of the epididymal proteins are modulated by androgen in either positively or negatively manner. Other 43% of the proteins are modulated by factors like estrogen, retinoids, temperature and so on. The rest of the 6% of the proteins are not affected or regulated by any currently known factors [6, 52].

1.4.2.1. Testicular regulation

Testicular factors flow into the epididymis involve in the control of the caput protein secretion [6]. According to Brooks, these factors contain both stimulatory and inhibitory components [53]. This suggestion is supported by the *in vivo* efferent duct ligation study as some proteins were disappeared after efferent ducts ligation and cannot

doi:10.6342/NTU201903813

be rescued by high dosage testosterone administration, indicating that those testicular factors are nonandrogenic and are likely proteinous rather than steroids [54, 55].

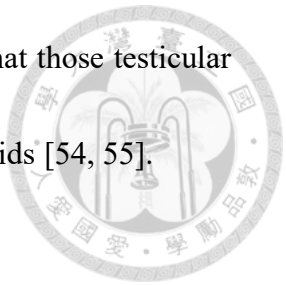

1.4.2.2. Androgen regulation

Testosterone and dihydrotestosterone (DHT) are the major androgens in the epididymis. Testosterone produced by Leydig cells in the testis will convert to dihydrotestosterone by 5-alpha-reductase in the epididymis [56]. Androgen can be delivered not only to the apical part of the epithelium through the epididymal flow, but it can also be delivered from the basal epithelium through the circulation [57]. Numerous studies have demonstrated that these androgens control the development and function of the epididymis in a concentration-dependent manner [58]. Besides relying on the luminal concentration of the androgens, the secretory activity of some epididymal proteins also depends on the expression of the steroid receptors such as androgen receptors (AR) and estrogen receptors (ER) on the surface [56].

1.4.2.3. Spermatozoa regulation

The testicular factors-dependent and androgen-dependent mechanisms likely regulate the majority portion of epidydimal proteins secretion [59]. However, spermatozoa *per se* has been shown to affect epididymal physiology and protein secretion [60]. For example, *in vitro* co-cultured of spermatozoa with specific regions

doi:10.6342/NTU201903813

of primary bovine epididymal cells stimulated the protein secretion [61]. It proves that spermatozoa can act as a lumicrine factor and initiate the effects on epididymal protein secretion via interactions with the epididymal epithelium.

doi:10.6342/NTU201903813

1.5. **Aim of this thesis**

As secretory QSOX1 isoform, QSOX1c is the dominant isoform in the mouse epididymis. The aim of this thesis is to investigate the regulatory stimulus for the secretion of mouse epididymal QSOX1. This may facilitate our understanding of the role of QSOX1 protein and its isoforms on the sperm physiology and the sperm maturation process in general.

doi:10.6342/NTU201903813

CHAPTER 2 Materials and methods

2.1. **Animals**

Experimental procedures involving the alive animals were conducted with the approval of IACUC protocols at National Taiwan University (Taiwan NTU-104-EL-00081). Specific pathogen-free outbred ICR mice were purchased from BioLASCO Taiwan Co., Ltd (Taipei, Taiwan). Mice were housed in the certified animal facility at the National Taiwan University Veterinary Hospital under the controlled-lighting regime (12 h light: 12 h dark), the temperature was maintained at 21-22 ℃, and supplied with food and water ad libitum.

2.2. **Tissue and protein sample preparation**

Mice were euthanized with CO_2 followed by cervical dislocation. Organs from male ICR mice were carefully dissected from fat and connective tissue, then separated for paraffin-embedded sample blocks and for protein analysis (for Western blotting). For paraffin block, organs were first fixed in 10% neutral buffered formalin on the shaker for 24 h (no longer than 48 h) at room temperature, standard dehydration and paraffin embedding procedures were followed and subsequently sectioned at 5 μm thickness for immunostaining processes.

doi:10.6342/NTU201903813

For Western blotting, protein samples were prepared as follows. To distinctively analyze the QSOX1 level in epididymis tissue and lumen, proteins from tissue and lumen fluid were separated. After removing the fat and blood vessels, mouse epididymis was punched by an 18G syringe needle in PBS on a temperature-controlled dissecting stage and further incubated for 5 min at 37 °C to allow the release of sperm cells from the epididymal lumen. Then the swim out sperm with epididymal fluid were collected as the epididymal fluid sample. Epididymis tissue without fluid was homogenized on ice in homogenization buffer (250 mM sucrose (Sigma-Aldrich, St. Louis, MO, USA), 1 mM EDTA (Sigma-Aldrich, St. Louis, MO, USA), 20 mM Tris/HEPES (Sigma-Aldrich, St. Louis, MO, USA), 1 % Triton X-100 (Sigma-Aldrich, St. Louis, MO, USA), pH 7.4) using glass homogenizer. Epidydimal fluid, tissue homogenates were supplemented with protease inhibitor (EDTA free cocktail tablet, Roche, Mannheim, Germany) and store at -80 °C until use.

To prepare whole-cell lysate of the epididymal epithelium cell line, the SV40-immortalized mouse caput epididymal epithelial (meCap18) stable cell line, a kind gift from Dr. Petra Sipila (Turku University, Turku, Finland), meCap18 was extracted with RIPA Lysis Buffer (AMRESCO, OH, USA) and supplemented with protease inhibitor (EDTA free cocktail tablet, Roche, Mannheim, Germany) and store at -80 °C until use.

doi:10.6342/NTU201903813

2.3. **Stable cell line culture**

MeCap18 were cultured in Dulbecco's Modified Eagle Medium, (DMEM, Gibco, USA) supplemented with 10% fetal bovine serum and 1% Antibiotic-Antimycotic (Gibco, USA). The cells were maintained in a humidified incubator at 37℃ with 5% CO_2. Immortalized Mouse Distal Caput Epididymal Epithelial Cell Line (DC2, Applied Biological Material Inc., BC, Canada) were cultured in Iscove's Modified Dulbecco's Medium, (IMEM, Gibco, USA) supplemented with 10% fetal bovine serum and 1% Antibiotic-Antimycotic (Gibco, USA). The cells were maintained in a humidified incubator at 33℃ with 5% CO_2. For sub-culturing, cells were first rinsed twice in Dulbecco's Phosphate-Buffered Saline (dPBS) (Gibco) before being trypsinized with 0.25% trypsin. Cells were detached by incubation with trypsin for 15 min at 37℃. Cells suspension was collected and centrifuged at 1500 xg for 10 min, at 4℃. The cell pellet was subsequently resuspended with cell culture medium and seeded back to a new flask at a proper density according to the experimental requirements.

doi:10.6342/NTU201903813

2.4. **Immunofluorescent staining**

For paraffin slide staining, tissue sections were deparaffinized with 100% xylene, rehydrated with 100%-80% ethanol, and washed in deuterium-depleted water (DDW). Slides were subsequently transferred to 10 mM citrate buffer (pH 6.0) for heated-mediated antigen retrieval (HMAR) using a specialized microwave at 95ºC for 2 cycles of 5 min each. After deparaffinization, slides were permeabilized with 100% pre-cold methanol for 10 min at -20ºC. Permeabilized samples were rinsed twice with PBS, followed by a 1 h incubation in blocking buffer (5% BSA (Sigma-Aldrich) diluted in PBS) at room temperature. Sections were subsequently incubated with primary antibodies, anti-QSOX1 (1:100 in PBS, Abcam83712) for 1 h at room temperature and then overnight at 4ºC. After rinse 3 times with filtered PBS, slides were incubated with secondary antibody, donkey anti-rabbit Alexa594 (1:150 dilution in blocking buffer, Jackson ImmunoResearch) for 1.5 h at dark before further rinsed 3 times with filtered PBS. Finally, nuclei were stained with mounting medium in the presence of diamidino-2- phenylindole (DAPI) (Vector Lab, Orton Southgate, Peterborough, UK). Slides were observed and fluorescent images were taken under the Olympus IX83 epifluorescent microscopy (Olympus, Tokyo, Japan).

For cell staining, cells were first grown on the coverslips coated with Poly-L-lysine (Sigma, P4832) in a proper density (i.e. $2x10^5$ cells were seeded in each well in a 12-

doi:10.6342/NTU201903813

well plate and allowed further growing for 24 h). After cells reach an 80% confluency, they were rinsed twice with filtered PBS, fixed, and permeabilized with 80% acetone at -20ºC for 10 min. Fixed cells were dried in a ventilated hood before proceeding further for blocking for 30 min at room temperature using 1% filtered BSA. Standard immunostaining procedures were followed as mentioned above.

2.5. **Electrophoresis, SDS-PAGE, and Western blotting**

The concentration of all protein samples was quantified using the BCA Protein Assay Kit (Pierce Biotechnology, Rockford, IL, USA) following the manufacturer's protocols. The equal amount of total protein from each sample was mixed with 1X LDS sample loading buffer (Invitrogen) and 10% reducing agent (50 mM dithiothreitol, DTT, Invitrogen) and boiled for 10 min at 95°C in a dry bath. After denaturing the protein, samples were immediately vortexed to prevent further aggregation, briefly spin down, and cooled on ice before loading on the gel. Proteins were separated by an 8-15% gradient SDS-PAGE gel (gradient T-Pro EZ Gel Solution, T-Pro Biotechnology, NTC, TW) using Bio-Rad Mini-PROTEIN® electrophoresis system (Bio-Rad Laboratories Ltd., Hertfordshire, DX).

For SDS-PAGE protein gel staining, a highly sensitive method was used. SDS-PAGE was first fixed by fixation buffer (50% methanol, 7% acetic acid) twice for 30 min, then stained by SYPRO ruby gel stain (Invitrogen) for overnight at room

doi:10.6342/NTU201903813

temperature in dark. After SYPRO ruby stain, the gel was washed by washing buffer (10% methanol, 7% acetic acid) for 1 h to remove the excessive staining and visualized by ChemiDoc™ Imaging Systems (Bio-Rad).

For Western blotting, proteins on the SDS-PAGE gel were transferred onto a polyvinylidene difluoride membrane (Immobilon-P, Millipore, Billerica, MA, USA). After blocking with 5% milk (Difo skim milk powder, BD) dissolved in 1X TBST (5 mM Tris, 250 mM sucrose, pH 7.4 with 0.05% v/v Tween 20) for 1 h at room temperature on shaker, the membrane was washed once with TBST and further incubated with primary antibodies against QSOX1 (1:200) and GFP (1:500) for 1 h at room temperature, and then for overnight at 4 °C. For loading control, EEF2 (1:50000) and beta-actin (1:1000) were used and primary antibody incubation was carried out at room temperature for 1 h. Blots were subsequently incubated with secondary antibody for 1 h at room temperature, washed with TBST three times and protein signals were chemically developed by the Clarity™ Western ECL Blotting Substrates (Bio-Rad) and visualized by ChemiDoc™ Imaging Systems (Bio-Rad).

2.6. **Human QSOX1-eGFP plasmid construction**

The plasmid containing human QSOX1 (hQSOX1) nucleotide sequence was purchased from GenScript Corporation (Piscataway, NJ). The 2263 bp QSOX1

doi:10.6342/NTU201903813

sequence was cloned in pcDNA3.1(+)-P2A-eGFP vector by *BamHI/NotI* restriction enzymes. To amplify the plasmid, the hQSOX1-eGFP plasmid was transformed into One Shot TOP10 Competent E.coli (Invitrogen), and the bacteria were spread onto ampicillin containing LB agar plate and incubated at 37℃ for 12-16 h. Isolated single colonies were picked up and amplify in the LB broth containing ampicillin at 37℃ for 12-16 h on a constant rotating (255 rpm) shaker. The plasmid was extracted by QIAprep® Spin Miniprep Kit (Qiagen) according to the manufacturer's protocol. The concentration and the quality of the plasmid were determined by Picodrop Microliter UV/Vis Spectrophotometer (Pico p100, Hinxton, UK).

To validate the plasmid structure, the plasmid was cleavage by restriction enzyme BamHI-HF and NotI-HF. The cleaved vector and DNA fragment were separated by 1% agarose gel electrophoresis and visualized by ultraviolet illumination after ethidium bromide staining.

2.7. ***In vitro*** **hormone treatment assays and cell-spermatozoa co-culture assays**

2.7.1. Cell transfection

Human QSOX1-eGFP plasmid was chemically transfected to meCap18 and DC2 by Lipofectamine™ 3000 Transfection Reagent (Invitrogen). In brief, approximately $2x10^6$ cells were cultured with DMEM and IMEM (supplement with 10% FBS and 1%

doi:10.6342/NTU201903813

Antibiotic-Antimycotic) in 24-well plate for 24 h to reach 90% confluence. Thirty minutes before transfection, medium was refreshed. Standard transfection protocol and procedures were followed according to the manufacturer's instruction. 24 h after the transfection, transfection efficacy was evaluated by Olympus IX83 epifluorescent microscopy. To further validate the expression and secretion of hQSOX1-eGFP in transfected cells, the transfected cells proceed with indirect immunofluorescent staining as described above. Secretory hQSOX1-eGFP protein was detected by Western blotting using both anti-QSOX1 (Abcam) and anti-GFP (Invitrogen) from the collected medium.

2.7.2. Establishment of in vitro co-culture system

To establish the co-culture model, hQSOX1-eGFP protein secretion activity was first evaluated in the cell culture medium. hQSOX1-eGFP transfected cells were washed with dPBS to remove FBS and phenol red from the original culture medium. Phenol red and FBS free FluoroBrite™ DMEM medium containing 1% Antibiotic-Antimycotic was added to each well for further incubation. Cell culture medium was collected at different the time point (12, 24, 36, 48, and 60 h after incubation) and centrifuged at 3000 xg at 4°C for 10 min to remove the cellular debris. Fluorescent intensity correlated to the concentration of hQSOX1-eGFP in the medium was then measured by SpectraMax® M5 Multi-Mode Microplate Readers (Molecular Devices).

doi:10.6342/NTU201903813

Based on the fluorescent intensity accumulating curve allowing us to determine a treatment starting point, we chose the secretion plateau time point 48 h post-medium exchange (after changing medium into FluoroBrite™ DMEM), as our 1st treatment time point.

2.7.3. Androgen treatment assays

After the protein secretion of QSOX1-eGFP transfected cells reach a plateau in the absence of exogenous stimulation (at 48 h post-medium exchange), 5 nM, 10 nM, 20 nM, and 40 nM testosterone (Sigma-Aldrich, St. Louis, MO, USA) and DHT (Sigma, St. Louis, MO, USA) were respectively added into each well. To examine the effects of androgen, fluorescent intensity was measured at a 4 h interval.

2.7.4. Animal preparation and acquisition of epididymal spermatozoa

Adult male mice, (over 12 weeks of age), were used in this study. After euthanization with CO_2, mouse epididymides were removed immediately and bathed in pre-warmed Whitten's HEPES medium (100 mM NaCl, 4.7 mM KCl, 1.2 mM KH_2PO_4, 1.2 mM $MgSO_4$, 5.5 mM glucose, 1 mM Pyruvic acid, 4.8 mM Calcium L-lactate hydrate, 20 mM HEPES, PH 7.4). Spermatozoa from the caput and cauda regions were collected separately. Briefly, epididymides were subjected to the removal of fat and blood vessels under the dissecting microscopy on a Thermo controlled (37°C) working

doi:10.6342/NTU201903813

stage (Tokai HIT, Japan). To prevent the contamination of cells debris, an 18G needle was used to create pores on the epididymis tissue to allow spermatozoa swimming out of the epididymis. Sperm suspension was collected and further filtered through the 40 μm pore size Falcon™ Cell Strainers (Fisher Scientific), with a 15 min incubation for allowing motile spermatozoa to swim up at 37℃. Motile spermatozoa collected from the upper three-quarters of the suspension used to conduct further co-culture assay. The remain epididymal fluid was replaced to cell culture medium to prevent the epididymal fluid contamination. Direct interaction and indirect interaction assay were set up using Transwell® (Corning, 3470) with a 0.4 um pore size membrane (Fig. 7A).

2.8. **Proteomics analyses**

2.8.1. Sample preparation

To identify the potential protein candidates that are responsible for sperm-epithelium communication, culture medium from the co-culture system described above were collected. Without and with sperm co-culture groups were control and sample group. After removing the cell debris (centrifuged at 3000 xg for 10 min at 4℃), the medium was further concentrated via vivaspin concentrators with a molecular weight cut-off at 3000 kDa (GE Healthcare). To achieve sufficient concentration of the collected medium, the co-culture supernatant was centrifuged at 3260 xg at 4℃ until a

doi:10.6342/NTU201903813

15 to 30-fold decrease in sample volume was achieved. During the concentration procedures, both solvent and low molecular-weight solutes would flow through the membrane and the remaining proteins were collected from the upper side of the membrane. After resuspension of the concentrated medium, filtered PBS was used to gradually replace the concentration buffer. To visualize the differences between groups, electrophoresis was carried out and the SDS-PAGE gel was stained with SYPRO-ruby gel stain as mentioned above.

2.8.2. In-soluble digestion of proteins / MS analysis

For identifying the protein candidates that are being secreted into the medium upon sperm-epithelium co-culture experiments, LC/MS/MS was performed. Soluble protein samples were first denatured by reduction buffer (2 mM DTE / 8 M Urea) for 1hr at 37℃. Lys-C (1 h, 37℃) and Trypsin (16 h, 37℃) were subsequently used as the digestion enzymes, and the digested peptides were suspended in 0.1% formic acid and were desalted by zip tip. LC/MS/MS was performed using Orbitrap Fusion™ Tribrid™ Mass Spectrometer (Thermo Scientific™).

The mass spectra data files were analyzed using Mascot Daemon (version: 2.6.0; Matrix Science, London, UK) searched against the SwissProt Mus musculus protein database (dated: 5/17/2019). Only two missed cleavages were allowed and a MASCOT score ≥35 to identify proteins of interest (score: E-value <0.05 are reported). These

doi:10.6342/NTU201903813

protein IDs were converted into Uniprot gene ID for future categorization and molecule function annotation studies. Protein IDs that reach the above-mentioned requirements were first categorized into three major subgroups: (1) sperm origin, (2) epithelium/luminal fluid origin and (3) uncategorized based on published literature [62, 63].

2.8.3. Gene ontology (GO) analysis and network analysis

Following GO analysis, PANTHER (protein analysis through evolutionary relationships) (v14.1) was used to classify proteins based on their protein biological process and molecular function.

The protein network analysis was conducted using the Cytoscape (v3.7.1) with the addition of ClueGo plugin (v2.5.4) [64]. GO Biological Process Annotation (downloaded 27.02.2019) for caput sperm protein, epididymal lumen protein, and uncharacterized protein were compared for gene enrichment (right-sided hypergeometric test) using Benjamini-Hochberg multiple test correction. Network parameters were set as follows: GO Tree Levels (min = 3, max = 8), GO term restriction (min #genes = 5, min % = 4), and GO Term Connection Restriction (Kappa score threshold = 0.4). Only terms with a p-value ≤0.05 were shown.

doi:10.6342/NTU201903813

CHAPTER 3 Results

3.1 **Post-natal QSOX1 protein expression and secretion in the epididymis.**

To investigate the potential stimuli for post-natal QSOX1 secretion, epididymis tissue sections from 20, 30, 40, 50, 60, and 80-day-old ICR mice were subjected to immunofluorescent study using anti-QSOX1c antibody which can specifically detect secretory QSOX1c. The fluorescence micrographs illustrating the overall expression patterns of QSOX1c in the epididymis were presented in Figure 4. In the epididymis of the 20 and 60 day-old mice, only weak, but unified luminal QSOX1c signal was detected throughout the epididymis. In marked contrast, an increase in positive QSOX1c signal was detected in the lumen of the corpus segment of epididymis in 30-day-old mice and gradually shift toward to cauda segment of the epididymis in 40-day-old (Fig. 4).

To further quantify the dynamic changes of QSOX1c at different post-natal stages, Western-blotting analysis was carried out. As shown in Figure 5A-B, the QSOX1c signal was detected at 63kDa in both epididymis tissue homogenate and epididymal fluid extracted from the epididymal lumen, and the signal intensity was gradually increased along with post-natal development of the animal (Fig. 5A-B). As the total amount of QSOX1 protein increased in an older animal, to subjectively quantify the

doi:10.6342/NTU201903813

ratio of “secreted QSOX1 (i.e. QSOX1c)” at different developmental stages, the intensity of QSOX1c signal measured in the fluid was normalized with the intensity total QSOX1 signal in the whole tissue homogenates. As showed in Figure 5C, a two-fold (2.42 times) increase of QSOX1c protein in the epididymal lumen was detected in day 30 post-natal samples, and the signal became steadily afterward (Fig. 5C)

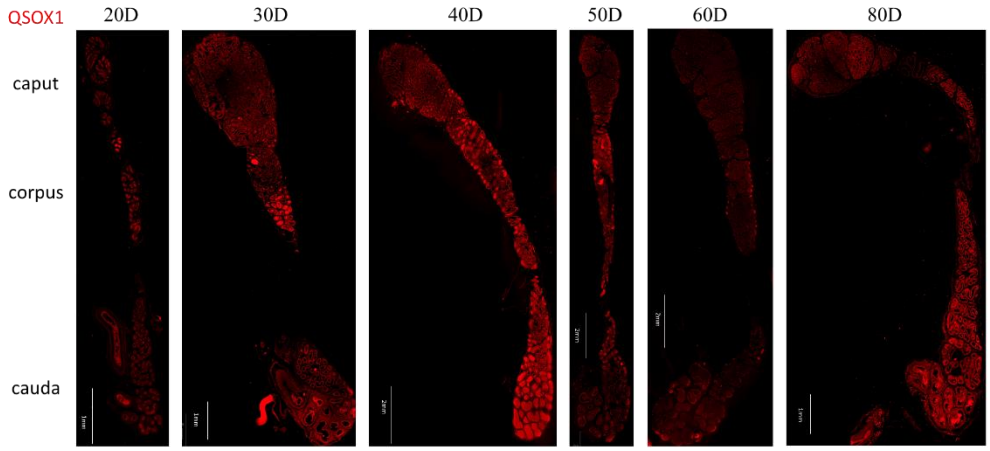

Figure 4. Detection of secretory QSOX1c in the mouse epididymis.

Epididymal tissue sections from mice of different post-natal (20,30, 40, 50, 60, 80 days) ages were subjected to anti-QSOX1c antibody examination. As shown on the left that from the top to the bottom of those images depicted three major epididymal segments, caput corpus and cauda, and positive QSOX1c was showed in red color.

doi:10.6342/NTU201903813

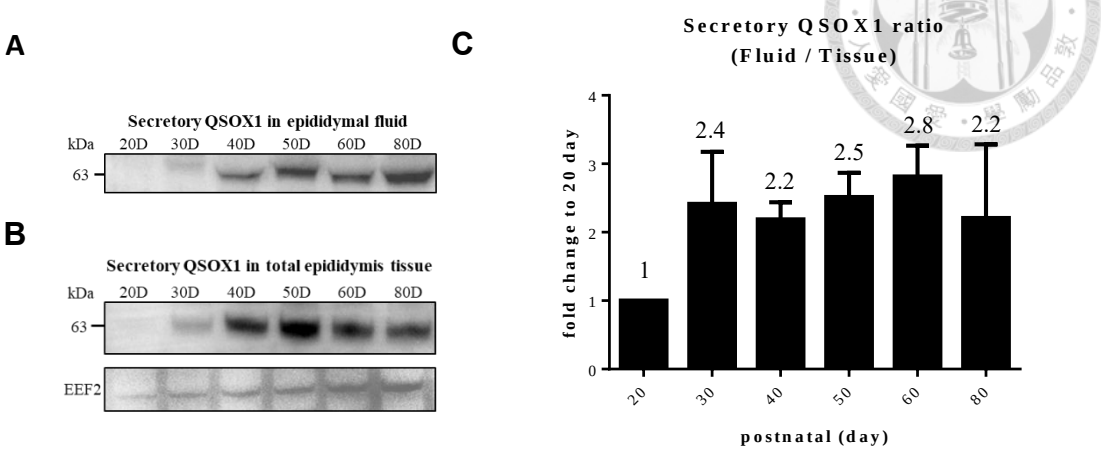

Figure 5. QSOX1 protein secretion ratio at different postnatal stages of mouse epididymis.

Protein samples were collected from the epididymis from 20, 30, 40, 50, 60, and 80-days-old mice (A) Distinct signal at 63kDa from the Western blotting results indicated secretory QSOX1c level in the epididymal fluid. (total protein loaded: 30μg) (B) Epididymis tissue homogenates (Total protein loaded: 30 μg) without epididymal fluid was analyzed by Western blotting. EEF2 as an internal control was used for loading control. (C) Ratios between secretory QSOX1 (QSOX1c) and total epididymal QSOX1 protein were quantified. X-axis indicated the post-natal age of the mice, and the Y-axis showed the fold change of Western-blotting signal as compared with those at day 20.

doi:10.6342/NTU201903813

3.2 **Successful QSOX1 overexpression system established for co-culture model.**

To demonstrate QSOX1 secretion behavior *in vitro* and to investigate potential exogenous stimuli for QSOX1 secretion, the transfected QSOX1-eGFP cell culture model was set up. The construction map was shown in Figure 4A. After transformation constructed plasmid into competent E.coli TOP10 cells (Invitrogen), positive colonies were selected for further DNA extraction. The structure of the plasmid was validated by restriction enzyme digestion which was expected to cleave *constructed vector* into two distinct bands at 6200bp (for *eGFP vector),* and at 2263bp (for *QSOX1)*. As showed in Figure 4B, the three chosen colonies all displayed two distinctive bands upon plasmid purification.

The corrected plasmid was then amplified by E.coli, and transiently transfected into meCap18 stable cell line to overexpress the QSOX1-eGFP fusion protein. As showed in Figure 4C, the cells were successfully transfected, and the QSOX1-eGFP fusion protein located at the same peri-nuclear cellular localization as the endogenous QSOX1 (Fig. 4D). The overexpression of QSOX1-eGFP fusion protein was further validated by Western blotting as a single protein band corresponded to the molecular weight of the QSOX1-GFP fusion protein was identified at 97kDa in the culture medium from transfected cells indicating the positive secretory activity of QSOX1-eGFP fusion protein (Fig. 4E).

doi:10.6342/NTU201903813

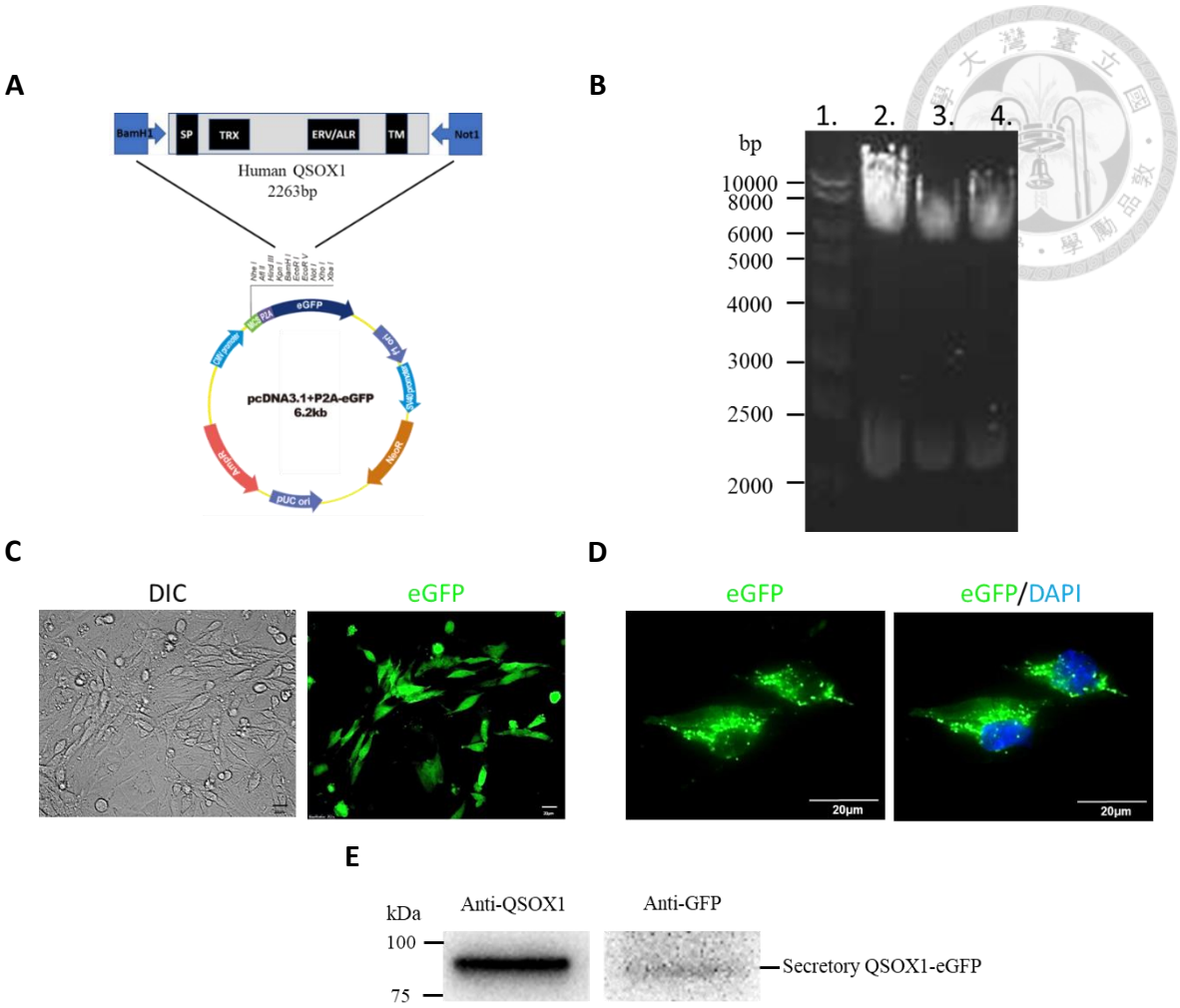

Figure 6. Plasmid construction of recombinant human QSOX1-eGFP and transfection results in the meCap18 stable cell line.

(A) The whole sequence of *human QSOX1* was subcloned into a *BamHI-NotI* restriction site in the *pcDNA 3.1-eGFP vector*. (B) Extracted DNA was separated by 1% agarose gel under 150mv for 40 mins. Lane 1: 1 K DNA ladder, lane 2-4: BamH1-HF and Not1-HF digestion products from three different E.coli colonies. (C) Low magnification images of meCap18 cells showed the transfection efficiency of QSOX1-eGFP fusion protein. (D) In line with known cellular localization of endogenous QSOX1, the QSOX1-eGFP fusion protein (shown in green) was distributed in the peri-nuclear cytosol of epididymal epithelium. (E) The western blotting analysis was applied to demonstrate the presence of QSOX1-eGFP fusion protein in the cell culture medium. Both QSOX1 and eGFP proteins were identified at the same molecular weight showing QSOX1-eGFP fusion protein can be secreted into the medium.

doi:10.6342/NTU201903813

3.3 *In vitro* co-culture system revealed regulatory stimulus for QSOX1 secretory

After validation on the secretion capability of QSOX1-eGFP fusion protein in transfected cell (Fig. 6E), we continued to investigate the regulatory mechanism underlying QSOX1 protein secretion using *in vitro* sperm-epididymal epithelium (meCap18) co-culture system. A schematic illustration on the experimental setup was shown in Figure 7. Transfected monolayer meCap18 secreting the fusion protein in the medium was used and culture medium was collected for the detection of fluorescent intensity which can be correlated with the secretory activity of QSOX1 upon stimulation. To minimize the detection and measurement bias from unstable QSOX1-eGFP secretion in the absence of exogenous stimuli, the starting time point for additional stimuli was first determined. 24 h after cell transfection, regular culture medium (with serum) was replaced by serum-free FluoroBrite™ DMEM (as time point 0) to maximize the detection of accumulative fluorescence intensity. As showed in Figure 7 (left panel), QSOX1-eGFP concentration was gradually increased during the first 36 h and became steady after 36 h post-medium exchange. Due to the experimental variability at 36 h (data are not shown), we considered 48 h time point was the most stable and appropriate time point for the addition of exogenous stimuli (e.g. hormones or spermatozoa).

doi:10.6342/NTU201903813

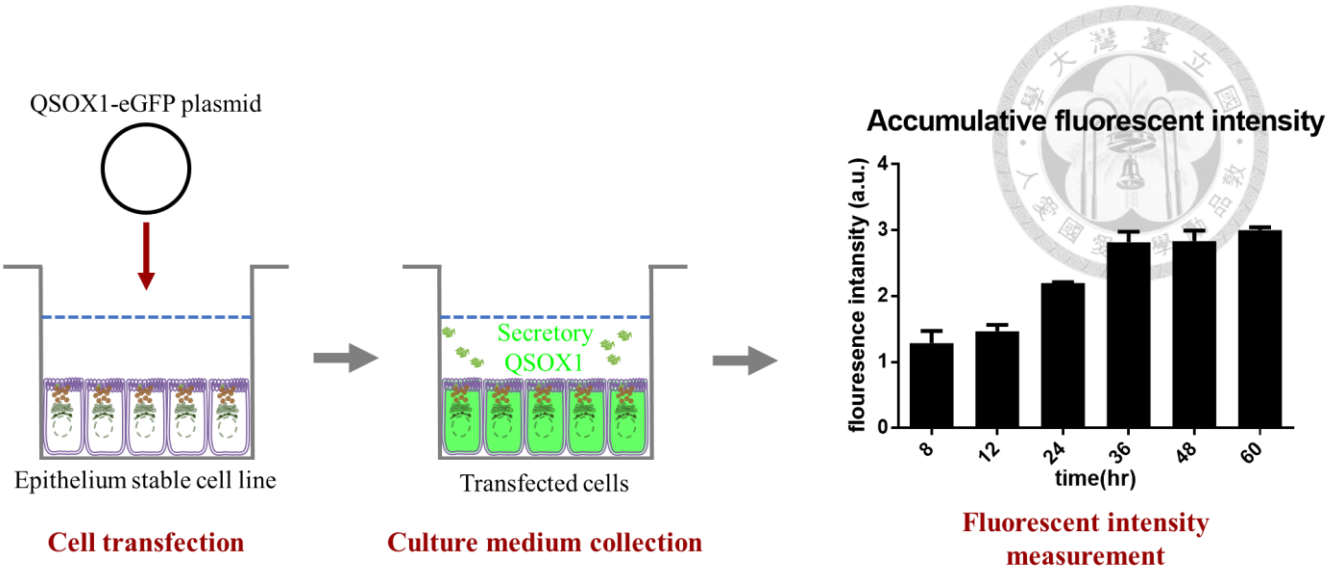

Figure 7. Illustration of procedures for the co-culture model and the measurement of secretory QSOX1.

Amplified QSOX1-eGFP plasmid was transiently transfected into meCap18. FluoroBrite™ DMEM was used for reducing autofluorescence and maximize the detection of the fluorescent signals. The eGFP fluorescent intensity which correlated QSOX1 concentration in the medium was measured at 8, 12, 24, 36, 48, and 60 h post-medium exchange. Data were represented as Mean ± SEM.

doi:10.6342/NTU201903813

3.3.1 Androgen showed little effects on QSOX1 secretion in epididymal epithelium cells

Two important events occurring at post-natal day 30 are the emergence of spermatozoa in the epididymal lumen and the 1st testosterone surge, to test the effects of androgen on epididymal QSOX1 secretion, transfected meCap18 cells and DC2 cells were separately treated with two most commonly seen forms of androgen: testosterone (T) and dihydrotestosterone (DHT). For data presented in this sets of experiments, the y-axis was expressed as fold change to control (without stimuli). The x-axis indicated the incubation time post-medium exchange as mentioned above. Both T and DHT were added into the medium at 48 h time point.

Based on earlier studies and measured physiological serum androgen concentration [65], 5 nM, 10 nM, 20 nM, and 40 nM testosterone and DHT were used. Androgen was added into cell culture medium at 48 h time point. As shown in Figure 8A, 12 h after co-incubation of testosterone (60 h time point), a significant increase (1.1-1.3 fold) in QSOX1 secretion was measured. When a different mouse epididymal epithelium stable cell line, DC2 was used, similar to that of meCap18 cell line, only little effect (~1.3 fold increase) on QSOX1 secretion was observed after 40nM testosterone treatment for 4 h (Fig. 8B); therefore, testosterone and DHT treatments only have little effects on QSOX1 secretion behavior under our *in vitro* experimental

doi:10.6342/NTU201903813

setup.

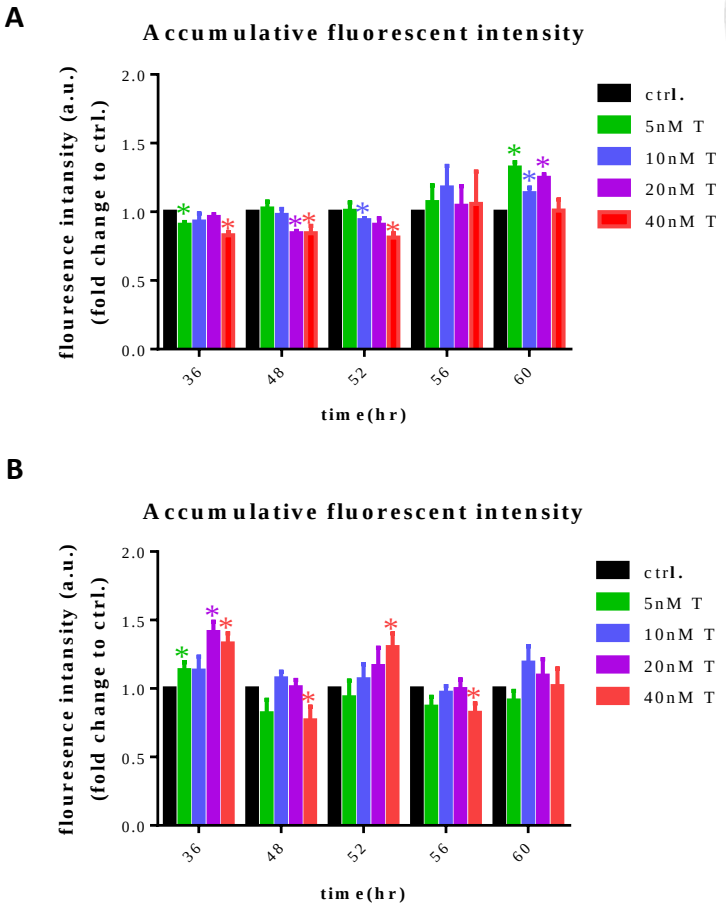

Figure 8. Effect of testosterone treatments on QSOX1 secretion behavior *in vitro.*

Actual raw values from each time point were normalized to the control group and expressed as fold change. Time points 36 h and 48 h were groups without any treatment. (A) Results of the effect of testosterone on meCap18. (B) Results of the effect of testosterone on DC2. Black bar: control (only transfected cells without testosterone). Green bar: 5 nM T. Blue bar: 10 nM T. Purple bar: 20 nM T. Red bar: 40 nM T. Data were represented as Mean ± SEM; *p < 0.05, in comparison with control; NS = no significant difference to control.

doi:10.6342/NTU201903813

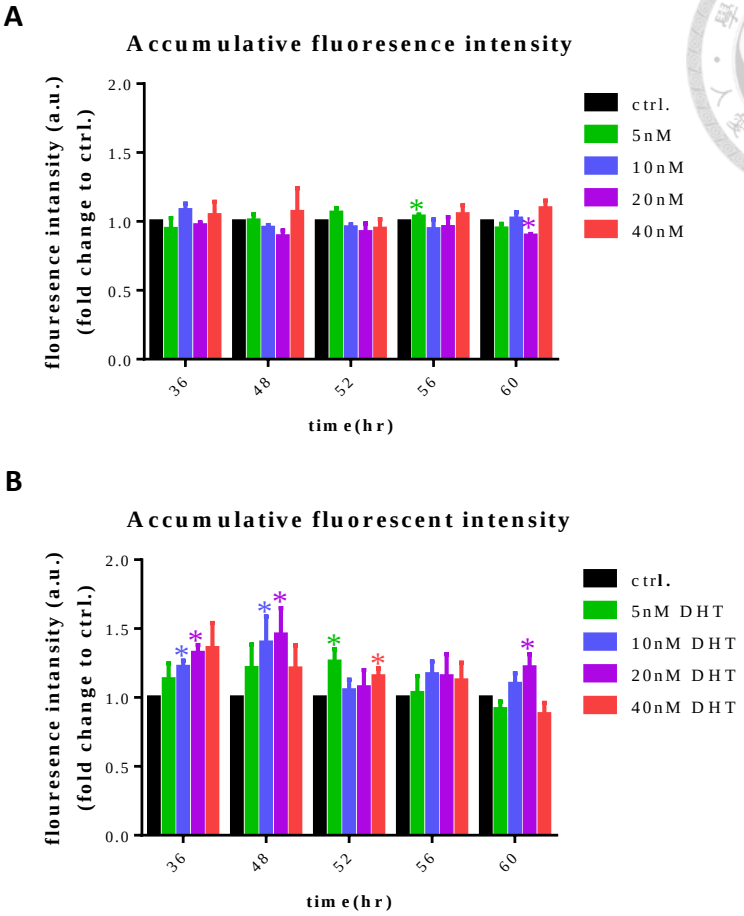

Figure 9. Effect of DHT treatments on QSOX1 secretion behavior *in vitro.*

Actual raw values from each time point were normalized to the control group and expressed as fold change. Time points 36 h and 48 h were groups without any treatment. (A) Results of the effect of DHT on meCap18. (B) Results of the effect of DHT on DC2. Black bar: control (only transfected cells without testosterone). Green bar: 5 nM DHT. Blue bar: 10 nM DHT. Purple bar: 20 nM DHT. Red bar: 40 nM DHT. Data were represented as Mean ± SEM; *$p < 0.05$, in comparison with control; NS = no significant difference to control.

doi:10.6342/NTU201903813

3.3.2 Spermatozoa facilitate QSOX1 secretion

Since spermatozoa is a potential candidate for regulating QSOX1 secretion in the epididymis. The sperm and meCap18 co-culture system were carried out to evaluate direct and indirect interactions. For the direct experimental setup, sperm cells recovered from either caput or cauda region was co-incubated with epididymal epithelium in which sperm cells can directly interact with the meCap18 (Fig. 10A). For indirect experimental setup, sperm cells were separated from meCap18 by Transwell® system to prevent direct physical contact with the meCap18 (Fig. 11A).

In the direct co-culture system, significant increase in QSOX1 secretion was observed after 4 h when 2 million caput sperm cells were co-incubated (Fig. 10B, red bars). When 1 million caput sperm cells were used, significant changes were detected after 8 h co-incubation (Fig. 10B, blue bars). The stimulation of QSOX1 secretion seemed to require a threshold number of sperm cells as adding 0.5 million sperm cells didn't facilitate QSOX1 secretion (Fig. 10B, green bars); moreover, QSOX1 secretion pattern also exhibited a time-dependent manner as showed in Figure 10B. To examine whether sperm cells of different maturation stages (e.g. caput sperm vs. cauda sperm) can elicit distinct QSOX1 secretion behavior, we also recovered cauda sperm cells for further direct co-incubation treatment. As showed in Figure 10C, only 2 million cauda sperm cells were able to result in significant secretion of QSOX1 after 8 h (time point

doi:10.6342/NTU201903813

56 h) of co-incubation (Fig. 10C).

To investigate whether sperm cells are able to stimulate epididymal QSOX1 secretion without direct physical interactions with the epithelium; in another word, whether sperm cells are able to stimulate epididymal QSOX1 secretion via secreting sperm-origin molecules, an indirect co-culture system using Transwell® separator with 0.4 um membrane pore size was applied (Fig. 11A). When 0.5, 1, and 2 million caput sperm were added into the upper chamber, QSOX1 level was 1.9, 2.3, and 4.9 times more than those of control at 4 h of co-incubation, 1.7, 1.7, and 3.1 times more than those of control at 8 h of co-incubation and 2.0, 2.1, and 3.6 times more than those of control at 12 h of co-incubation (Fig. 11B). In contrast, when cauda sperm cells were used, only 2 million cauda sperm cells can stimulate QSOX1 secretion, and the level of QSOX1 concentration detected in the medium was much lower (1.12 times more than control at 52 h time point and 1.17 times more than control at 56 h time point) than when caput sperm cells were used (Fig. 11C). During the sperm isolation processes, spermatozoa were isolated from standard swim-out process on the temperature-controlled stage, and epididymal fluid was further replaced by culture medium via centrifugation and washing step (1 time, 800g, 5min); however, it is still possible that remaining epididymal fluid may lead to misinterpretation of QSOX1 secretion in our *in vitro* study. To demonstrate the effects of epididymal fluid on QSOX1 secretion,

doi:10.6342/NTU201903813

meCap18 was incubated with epididymal fluid in the absence of sperm cells. As show in Fig. 11D, after epididymal fluid incubation for 12 h, a minor increase of QSOX1 level (1.4 fold) was detected when compared with control group; however, the fold change was minor when compared with experimental group in the presence of spermatozoa(3.3 fold) (fig. 11D).

doi:10.6342/NTU201903813

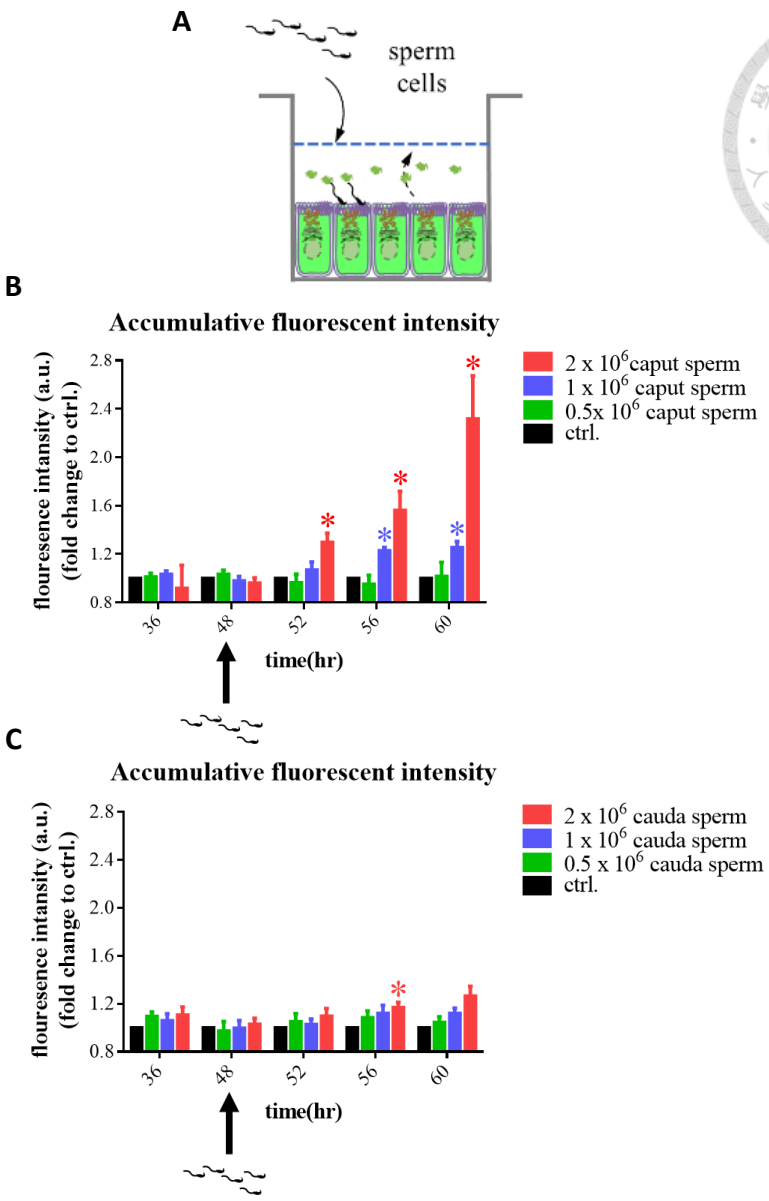

Figure 10. Effect of different mature status spermatozoa on QSOX1 secretion in direct co-culture system.

(A) Schema of direct co-culture systems. (B) Results of QSOX1 secretion from direct co-culture system using caput spermatozoa. (C) Results of QSOX1 secretion from direct co-culture system using cauda spermatozoa. (B-C) X-axis: transfected cell incubation time after changing the medium into Fluorbrite DMEM; y-axis: fluorescent intensity which corelated to QSOX1 concentration. Black bar: control group, only transfected cells; green bar: 0.5 million spermatozoa treatment; blue bar: 1 million spermatozoa treatment; red bar: 2 million spermatozoa treatment. Data were

doi:10.6342/NTU201903813

represented as Mean ± SEM; *p < 0.05, in comparison with control; NS = no significant difference to control.

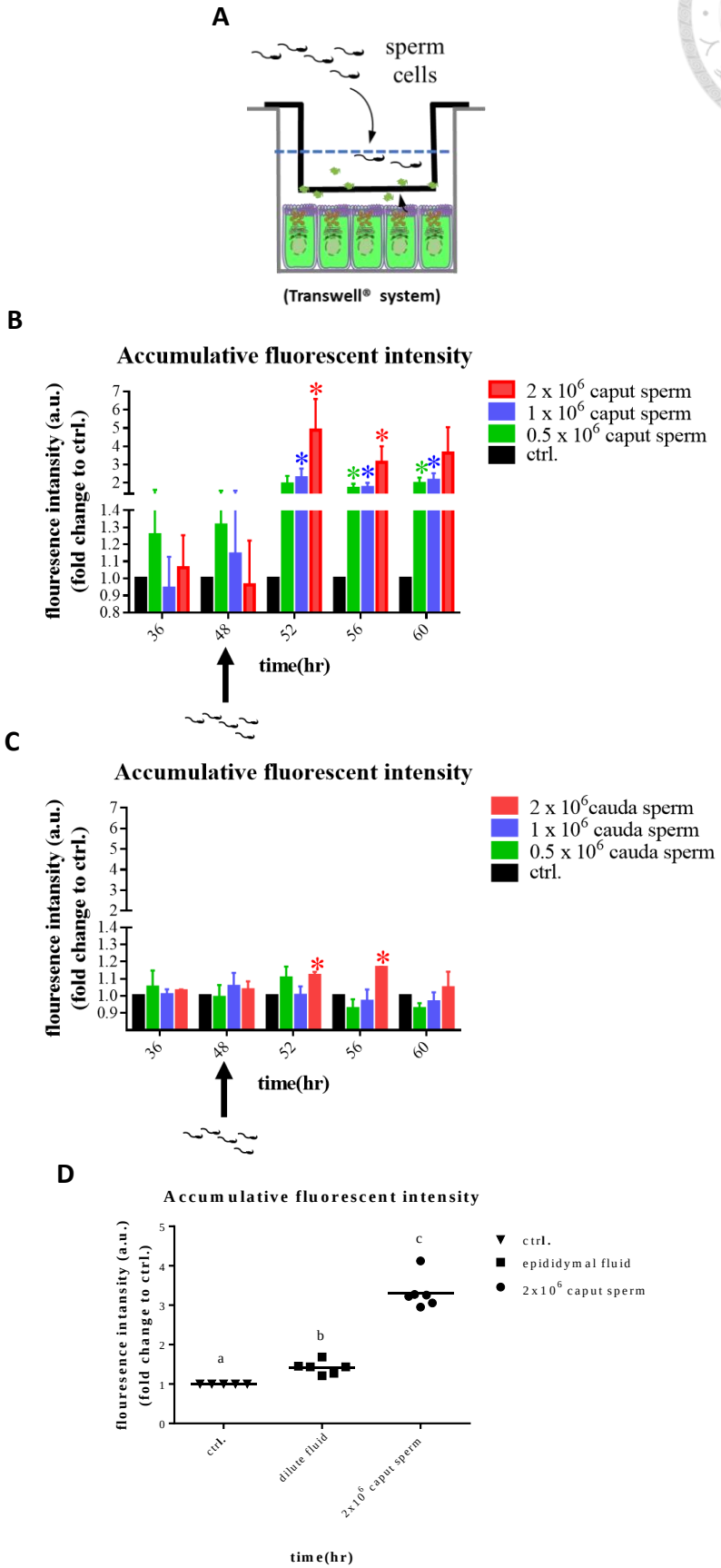

doi:10.6342/NTU201903813

Figure 11. Effect of different mature status spermatozoa on QSOX1 secretion in indirect co-culture system.

(A) Schema of indirect co-culture systems. (B) Results of QSOX1 secretion from indirect co-culture system using caput spermatozoa. (C) Results of QSOX1 secretion from indirect co-culture system using cauda spermatozoa. (D) The effects of epididymal fluid on mecap18. (B-C) X-axis: transfected cell incubation time after changing the medium into Fluorbrite DMEM; y-axis: fluorescent intensity which corelated to QSOX1 concentration. Black bar: control group, only transfected cells; green bar: 0.5 million spermatozoa treatment; blue bar: 1 million spermatozoa treatment; red bar: 2 million spermatozoa treatment. Data were represented as Mean ± SEM; *$p < 0.05$, in comparison with control; NS = no significant difference to control.

doi:10.6342/NTU201903813

3.4 Spermatogenesis defect *(Elp1$^{-/-}$)* mouse showed low level of epididymal QSOX1 protein expression.

To further investigate the effect of sperm on QSOX1 protein expression and secretion, well-established *Cre/loxP* system was used for generating sperm null knock out mouse. As described in earlier publication, *Vasa* as the promoter can specifically express Cre protein in germ cells which can give rise to germ-line specific knockout animal when mated with *loxP* site flanked animals. In this study, *Elp1*(also known as *IKBKAP* [inhibitor of kappa light polypeptide gene enhancer in B-cells, kinase complex-associated protein] in mouse) is a critical gene in meiosis process was flanked by two *loxP* sites. After recombination, the spermatogenesis process was disrupted in *Vasa-Cre* and *Elp1$^{flx/flx}$* animal and is characterized with the absence of sperm cells in the epididymis (In collaboration with Dr. Fu-Jung Lin at Department of Biochemical Science and Technology, NTU). As shown in Figure 12, the epididymis from wild type mouse and *Elp1* knock-out mouse were homogenized for Western-blotting analysis, and the data indicated that *Elp1* knock out mouse exhibited low level of secretory QSOX1c, suggesting the role of spermatozoa on the protein expression of epididymal QSOX1c (Fig. 12).

doi:10.6342/NTU201903813

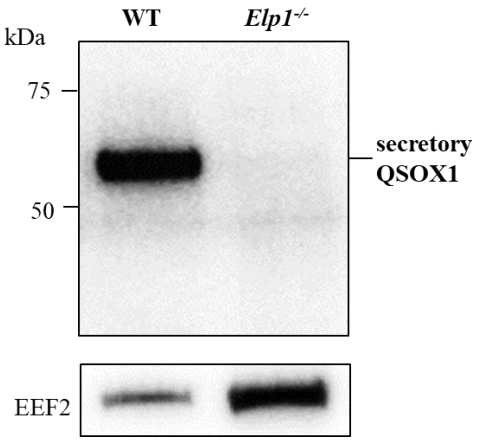

Figure 12. QSOX1c expression in *Elp1* knock out mouse epididymis.

Anti-QSOX1c antibody was used to detect secretory QSOX1 in the spermatogenesis defect transgenic animal. A single band at 63 kDa was observed in wild type mouse epididymis, but not in *Elp1*$^{-/-}$ mouse. EEF2: internal control; total protein loaded: 35ug/well.

doi:10.6342/NTU201903813

3.5 **Proteomic analysis**

To identify different molecule present in the culture medium, 1-D SDS-PAGE was first performed. Culture medium from both with or without sperm group were first concentrated, and protein concentrations were determined as above-mentioned, 90ug of total protein was loaded into each well and separated by electrophoresis. Sypro ruby (Invitrogen) was used to visualize the differences, a set of protein signals around 20-25kDa was observed exclusively from the medium containing sperm cells (Fig. 13A); however, due to the poor resolution of in gel-staining, in solution protein analysis was further performed.

LC/MS/MS identified 1358 and 1871 protein IDs in the control and treatment group, respectively (Fig. 13B). Based on selection criteria mentioned in the Materials and Methods section (two missed cleavages were allowed, and a MASCOT score ≥35), we further selected 582 proteins of interest (Fig. 13B, small green circle) for future analyses. Compared with proteome database published by recent papers [62, 63], those 582 protein IDs can further be classified into three groups: caput sperm origin protein (majority part for further analysis, see table 1 for the complete list of 258 protein IDs), epididymal epithelium origin protein, and uncharacterized protein (Fig. 13C).

Proteins of different origin (sperm, epididymal epithelium, and uncategorized) were subjected to bioinformatic analysis. To analyze the functions of these protein, GO

doi:10.6342/NTU201903813

annotation approach was used; to analysis the potential biological involvement of these proteins, biological process analysis was applied. Processes related to biological adhesion, cellular component organization or biogenesis, cellular process, developmental process, immune system process, localization, metabolic process, multicellular organismal process, reproduction response to stimulus were observed in all of the three groups. However, cell proliferation was only observed exclusively in uncharacterized group of proteins (Fig. 14A). The results of molecular function annotation indicated that binding activity and catalytic activity were the top two main functions of these proteins (Fig. 14B)

In order to study the correlation of these 582 proteins, a comparative network analysis was conducted to find GO Biological Process terms enriched in each group (Fig. 15). Terms with caput sperm protein, epididymal fluid protein and uncharacterized protein were shown in orange, blue and green respectively. The correlation of those proteins was performed by the overlapping of the terms and the edge distance. Proteins identified as caput spermatozoa origin showed specific terms like mitochondria biological processes, Golgi vesicle transport, regulation of apoptosis. Proteins that are categorized as luminal fluid specific protein involved in the regulation of receptors, negative regulation of protein complex assembly. For those of uncharacterized proteins, most of them were related to the regulation of RNA processes. Although the majority

doi:10.6342/NTU201903813

of the 582 proteins were involved in metabolic processes and catalytic processes, some proteins showed in all clusters are related to sperm fertility, motility and chromatin assembling. As the GO analysis is for predicting protein functions, proteins involved in stimulating QSOX1 secretion can be predicted. The top3 pieces of GO biological process ontology for caput sperm group described cellular process, localization, and metabolic process. Proteins in those terms had catalytic activity or involved in transport events (Fig. 16). The predictions were described in chapter 4.

doi:10.6342/NTU201903813

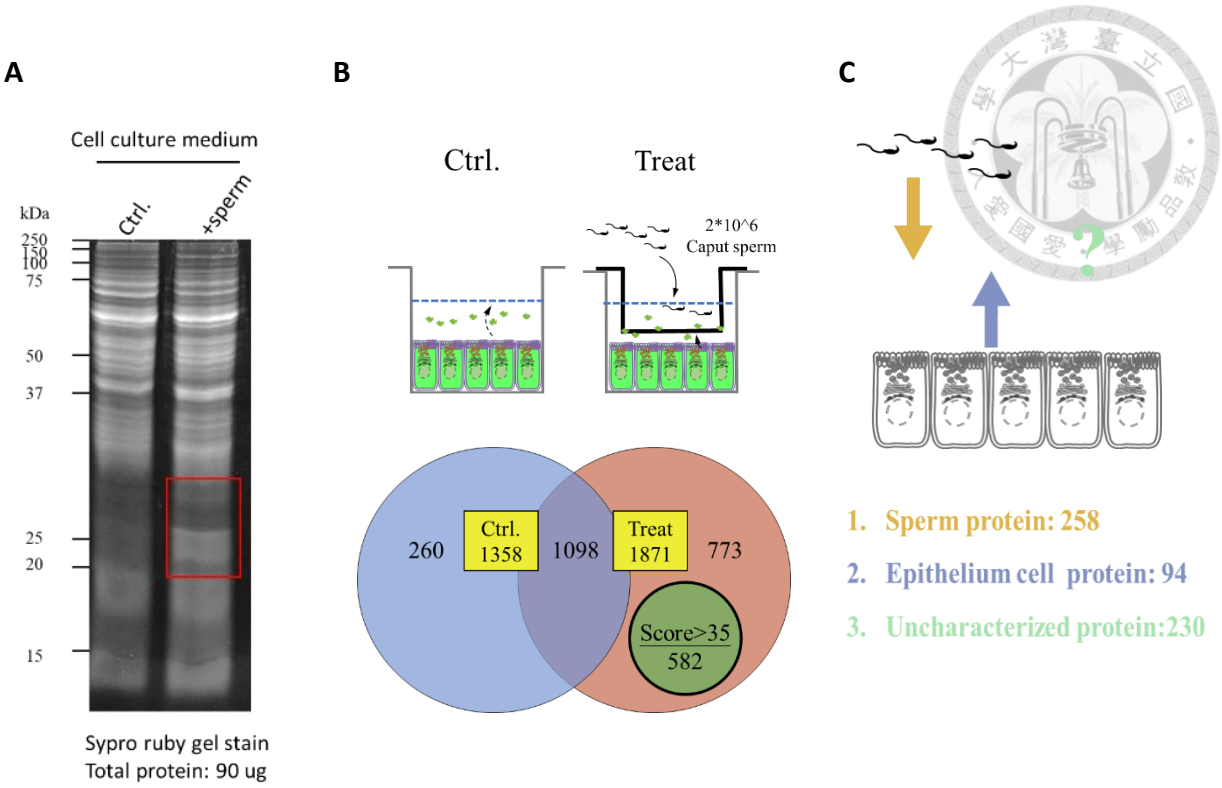

Figure 13. Summary of proteomic analysis.

(A) Representative 15% Sypro Ruby-stained gel. Left panel: culture medium from control group (transfected meCap18 cell); right panel: culture medium from sperm treated group (B) Mass spectrometry identified 1358 and 1871 protein IDs in control (Ctrl.) and sperm-treated (Treat) group, respectively. Venn diagram illustrating the overlapping relationship of protein identification between control and treatment groups. Among 773 proteins that were exclusively presented in treatment group, 582 proteins reached the selection criteria of MASCOT scoring ≥35 (showed in green). (C) Those 582 unique proteins presented in sperm co-culture medium were classified based on their origins. 258 proteins were classified as caput sperm proteome (orange arrow), 94 proteins belonged to epididymal epithelial proteome (blue arrow), and 230 proteins were uncharacterized.

doi:10.6342/NTU201903813

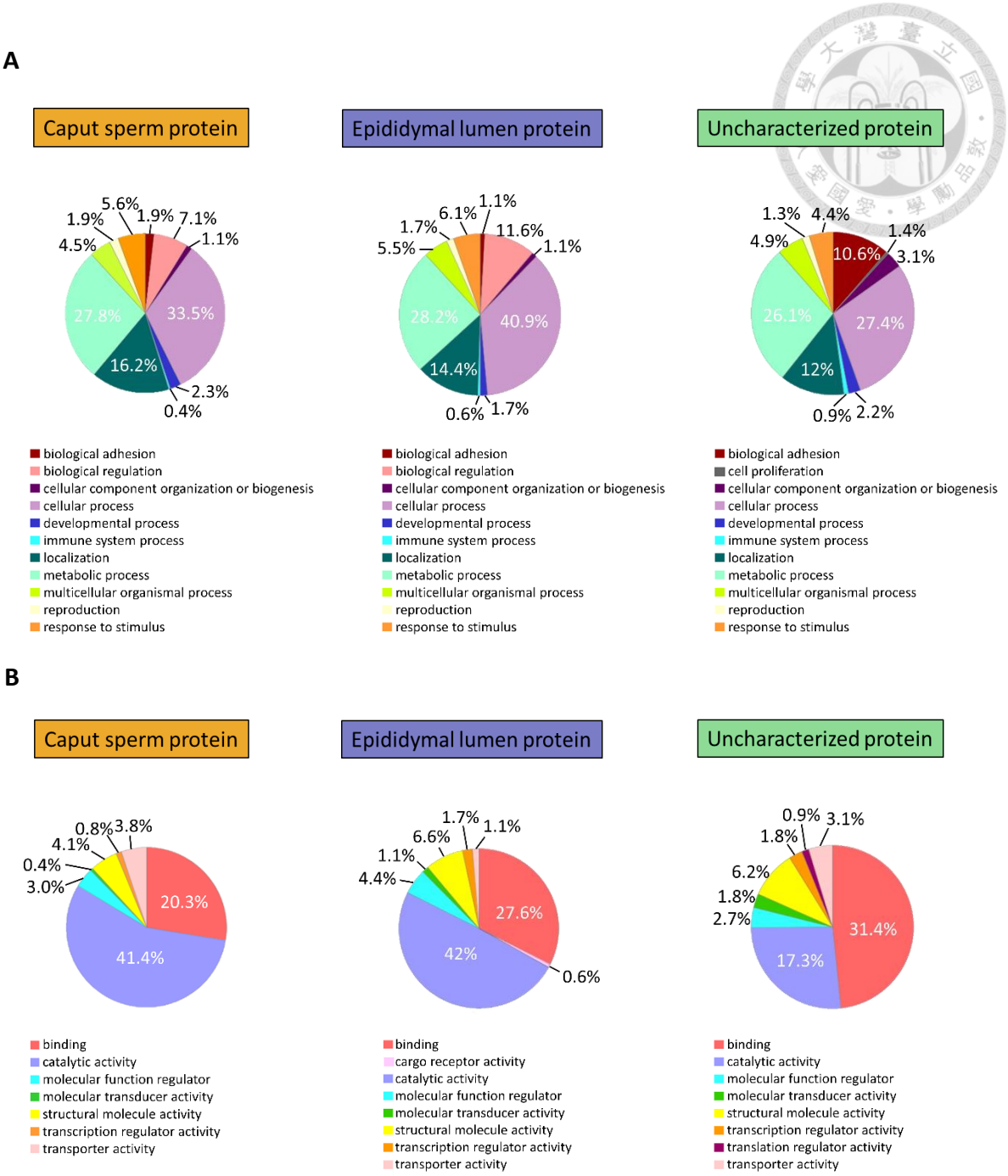

Figure 14. GO analysis performed using PANTHER (v14.1).

Panther gene ontology (GO) analysis for differentially enriched proteins in caput sperm protein group, epididymal lumen protein group, and uncharacterized group. (A) Enriched proteins in different groups were classified in different categories based on the biological processes, and (B)were also classified based on the molecular functions.

doi:10.6342/NTU201903813

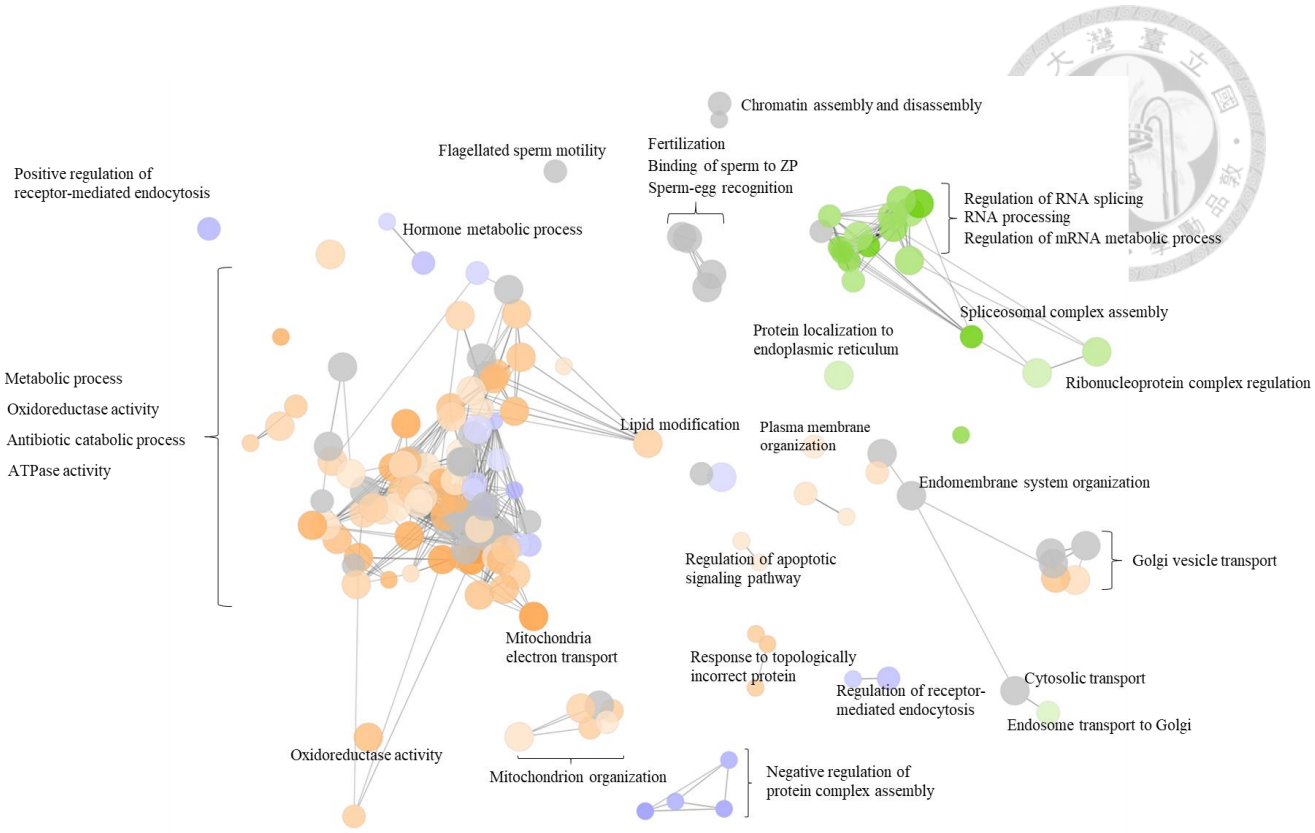

Figure 15. Enriched biological process GO annotation clusters distribution view.

Diagram indicating functional enrichment of GO categories for caput sperm group (in orange), fluid protein group (in blue) and uncharacterized protein group (in green) Functionally grouped network with terms as nodes linked based on their kappa score level (≥0.4). The node size represents the term enrichment significance. Functionally related groups partially overlap. No difference in grouped terms are shown in gray.

doi:10.6342/NTU201903813

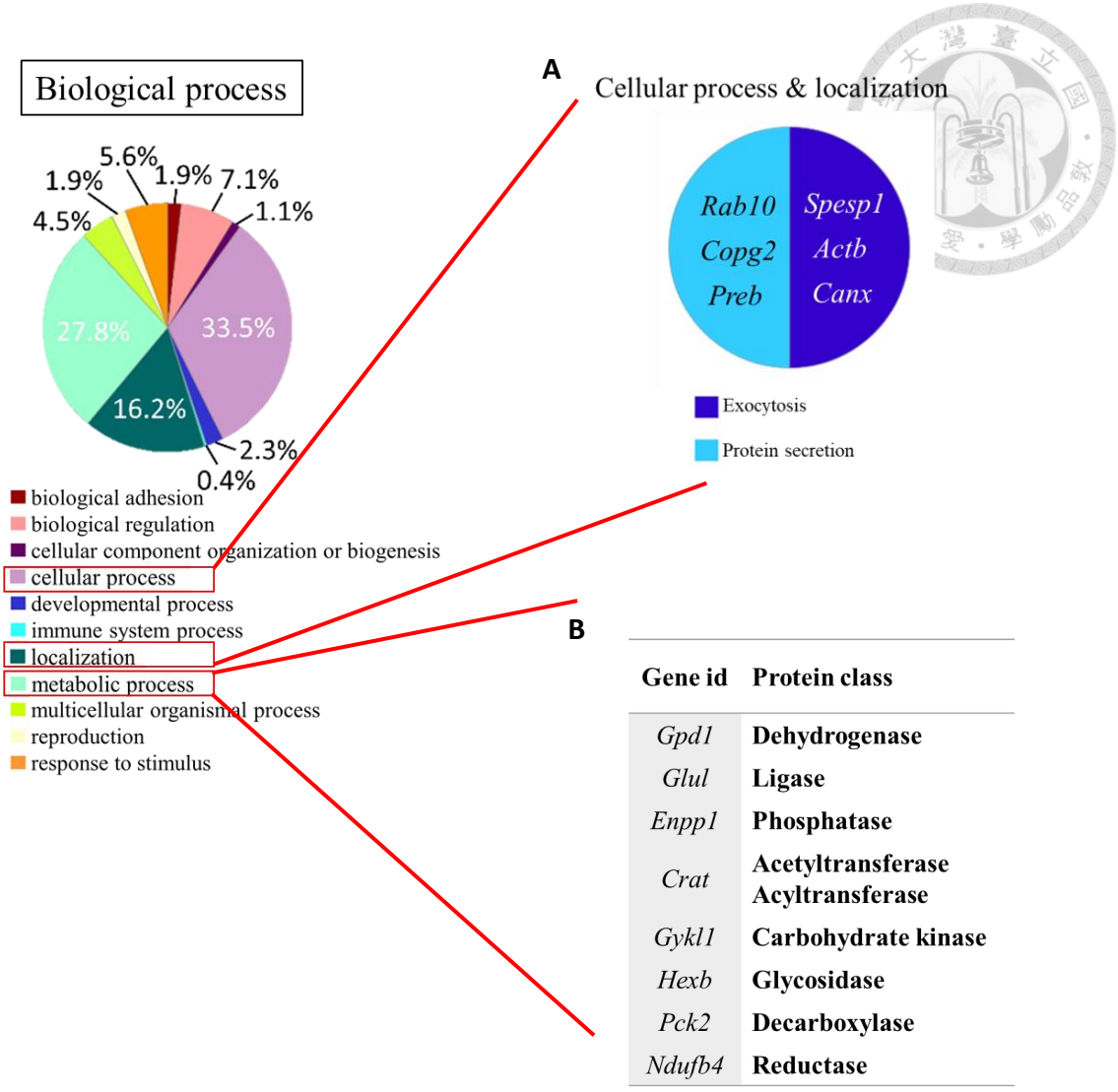

Figure 16. Proteins classified in the top3 sub-class terms of the biological process ontology.

The top3 pieces of GO biological process ontology for caput sperm group. (A) Under the cellular process and localization was 6 proteins involved in secretion and exocytosis events. (B) The majority of the metabolic process was enzyme.

doi:10.6342/NTU201903813

Chapter 4. Discussion

The mammalian epididymis supplies a complex microenvironment necessary for sperm maturation [66]. Regional variations in the epithelium gene and luminal protein profiles have been described in several species, such as the rat [67], mouse [68], boar [69], and human [70]. The observed diversity is partly owing to the dynamic and constant processes of absorption and secretion by the epididymal epithelium cells [71]. The specificity of the epididymal secretion at each epididymal segment is gradually established during postnatal development [72]. For example in mouse, the differentiation of the epididymal epithelium starts in the caput region around 2 weeks after birth, and followed by the corpus segment at 3 weeks and finally, the cauda regions around 4 weeks [73]. It has been shown that postnatal epididymal protein secretion is dynamic and under specific regulation at different postnatal development time point [74], in line with this, we observed that QSOX1 secretion activity was significantly increased at postnatal day 30 suggests that QSOX1 secretion might be regulated by specific luminal stimuli at around postnatal day 30.

Androgens (primarily testosterone and its more active metabolite dihydrotestosterone (DHT)) are the major group of hormones that control epididymal biological processes, such as differentiation and the function of the epididymal epithelium [75, 76]. However, other factors, such as testicular factors or spermatozoa

doi:10.6342/NTU201903813

may also be involved in the regulation of epididymal protein secretion [60, 77]. Among those potential regulatory factors, 1st androgen surge and the emergence of sperm in the epididymis are critical events occurring at postnatal day 30 [78-81]. To test the androgen effects, two cell lines were used in the *in vitro* evaluation system. Hormone requires its corresponding surface receptor to initiate cellular effects, due to limited androgen receptor expressed in the meCap18 stable cell line [82], it might not efficiently stimulate the QSOX1 secretion in meCap18 cells. To overcome these potential reasons, another mouse epididymis epithelium cell line called DC2 (distal caput epididymal epithelial cells), which show normal expression of androgen receptor on cell surface [83], was also used for androgen stimulation test. We observed that testosterone and DHT (ranged from 5-40 nM) treatments showing little effects on QSOX1 protein secretion behavior (compare to spermatozoa stimulation results) in both meCap18 and DC2, suggesting that androgens, at least testosterone, and DHT may not be the major regulators for QSOX1 secretion in the epididymis.

The essential role of epididymis on the maturation process of sperm cells has been studied intensively in the past decades; while most of the studies focused on uni-directional influences of the epididymal epithelium to sperm, whether sperm cells can actively participate in the regulation of epididymis biological processes is poorly understood. Nevertheless, the effect of sperm cells on the epididymal epithelium is

doi:10.6342/NTU201903813

likely occurring at different levels. For example, epididymis basal cells number decreased and expressed fewer F4/80 antigen when spermatozoa were absent from the proximal lumen [84]. Moreover, Carlos et al. demonstrated that co-incubation of the epididymal epithelium with spermatozoa enhanced epididymal protein secretion and greatly changed the pattern of secretory protein expression in caput cells [61]. In order to investigate the effect of spermatozoa on QSOX1 secretion, an *in vitro* co-culture system was established. Spermatozoa and epithelium co-culture has been described in much literature to study the relationship between spermatozoa and reproductive tracts [85-88]. For example, in 1992, Klinefelter described a Transwell® co-culture system that separated rat spermatozoa and primary rat epididymal epithelium cells [89]. In this study, to investigate the effects of sperm cells on the epididymal epithelium, spermatozoa were co-incubated with meCap18 stable cell line using both direct co-culture and Transwell® indirect co-culture systems. From the direct co-culture system, both caput and cauda sperm can facilitate QSOX1 secretion, and under our experimental setup, we observed caput sperm cells were more efficient and more potent than that of cauda sperm. This is likely due to the fact that when compared with cauda sperm cells, proteins on the surface of caput sperm are less stable and require QSOX1 to facilitate intra-molecular disulfide bond formation to stabilize their structure. The other reason could be the region specific bioreaction, those cauda sperm need to

doi:10.6342/NTU201903813

specifically stimulate cauda epithelium instead of caput epithelium.

The possible stimulatory mechanisms underlying our observed QSOX1 secretion could due to either direct physical contact of spermatozoa *per se* to the epithelium or from the indirect stimulation of proteins and molecules that are being secreted/shed from sperm cells. To investigate the later possibility, spermatozoa were separated by Transwell® system as described earlier [89]. Compared to cauda sperm, QSOX1 secretion was significantly increased under caput sperm stimulation supporting our earlier speculation that caput sperm may require more QSOX1 to facilitate their surface modification than those of cauda sperm. Interestingly, we observed that the amount of QSOX1 secretion in the indirect caput sperm co-culture system was about 3 times more than the direct caput sperm co-culture system. These results suggested that (1) sperm can alter epithelium behavior via direct contact [90] and may have negative effect on QSOX1 secretion in epididymis, (2) sperm cells can stimulate QSOX1 secretion without direct physical interaction with the epididymal epithelium, likely due to their active shedding off proteins and molecules upon the transit in the epididymis, and the shed proteins and molecules from sperm cells might be more efficient to stimulate QSOX1 secretion in the epididymis; however, detail mechanism and exact regulation require further investigation.

As we hypothesized that sperm cells can actively secrete or passively shed off

doi:10.6342/NTU201903813

proteins and molecules that subsequently stimulate QSOX1 secretion, the co-culture medium from the lower chamber of indirect Transwell® system was collected from for proteomic analysis. Many proteomic approaches have been described to identify protein candidates, for instance, one-dimensional and two-dimensional differential gel electrophoresis gel staining, protein microarrays, and Mass spectrometry-based method [91]. Among those that have been described, the liquid chromatography (LC)-MS or tandem MS (MS/MS)-based proteomics technologies provides highly sensitive analytical capabilities for generating proteomic profiles [92]. From our 1-D protein gel staining, a set of additional protein signal was detected in the medium when sperm cells were added; however, due to the low resolution of this approach, LC/MS/MS was conducted to identify the complete proteome profile in both control and sperm-treated groups. LC/MS/MS identified 1358 and 1871 proteins in the control and treatment group, respectively. After subtracting protein IDs that were identified in both groups, 582 candidate proteins were exclusively presented in the sperm-treated group. Among these 582 proteins that were detected from the lower chamber of indirect Transwell® system, some may be the proteins released by spermatozoa (and passed through the pored membrane), some may be the proteins secreted by meCap18 which were stimulated by spermatozoa. Based on comparative proteomics with previous studies that have characterized the mouse caput sperm proteome and caput lumen fluid

doi:10.6342/NTU201903813

proteome, these 582 proteins were classified into three groups: caput sperm protein, epididymal epithelium protein, uncharacterized protein. A previous study of the mouse caput sperm proteome 258/582 proteins and 94/582 proteins were classified into caput sperm protein (sperm origin) and epididymal epithelium protein (epididymal epithelium origin), respectively; the rest of 230 proteins were classified as uncharacterized protein (unknown origin) in this study.

In recent years, bioinformatics, protein network analysis, functional annotations, and pathway information advance the phenotype characterization of identified protein IDs [93]. Based on our data, a number of GO categories are enriched specifically in the caput sperm proteins group, epididymal epithelium protein group, and uncharacterized protein group. Gene set enrichment analysis was developed to classified the major protein profile in each group. Moreover, top 3 biological processes showed up in all three groups were a cellular process (e.g. metabolic process, cellular component organization, cellular response to stimulus), metabolic process (e.g. cellular, organic, primary metabolic process) and localization (e.g. cellular localization, the establishment of protein localization, macromolecule localization). To our specific interest, caput sperm origin proteins in culture medium involved in those top3 ontology could be the stimuli in the regulatory pathway of QSOX1 secretion.

The biological processes on the establishment of localization are known to

doi:10.6342/NTU201903813

participate in exocytosis, vesicle budding from membrane vesicle fusion and vesicle-mediated transport to the plasma membrane. These results suggested that "localization proteins" in the co-culture medium might involve in regulating the trafficking of epididymal secretory proteins. The results of molecular function annotation indicated that binding activity (including protein binding, heterocyclic compound binding, small molecule binding) and catalytic activity (including hydrolase activity, oxidoreductase activity, transferase activity) were the top two main functions of these proteins. In the network analysis result, the main group of proteins from caput sperm and epithelium were classified in the metabolic process, suggested that QSOX1 secretion regulation might be related to sperm metabolic process, and maybe upregulated by the metabolic by-products released from sperm cells.

To look more details on the proteins classified in the top3 biological process of caput origin protein group, there are 6 proteins participated in protein trafficking or fusion events. The predicted relationship of those proteins and QSOX1 secretion is shown in Figure 17. After released by sperm, those protein can directly reach to the epithelium cells and trigger QSOX1 secretion, or the membrane fusion protein can indirectly stimulated QSOX1 secretion by helping vesicles (containing stimuli) fusion to epithelium membrane (Fig. 17). In the top3 biological process ontology, proteins with catalytic activity behavior are the main group of proteins. The predicted

doi:10.6342/NTU201903813

relationship of those enzymes and QSOX1 secretion is shown in Figure 18. Antoher possibility for QSOX1 secretion might be that epididymal sperm releases factors that subsequently stimulate metabolic processes of epithelium and indirectly stimulate or accelerate the secretion of QSOX1 from the epididymal epithelium (Fig 18, lower panel).

In conclusion, based on our *in vitro* co-culture model, androgens are not the major stimuli for QSOX1 secretion; however, the QSOX1 secretion level was up-regulated in the presence of spermatozoa indicated that epididymal spermatozoa can facilitate QSOX1 secretion. Although we have identified some specific molecules originated from spermatozoa which might be the potential stimuli for QSOX1 secretion, the exact mechanism and molecules involved in the regulation of epididymal QSOX1 secretion require further studies. Future works should focus on functional study targeting specific molecules identified in the medium (especially those of sperm origin) to demonstrate the regulatory mechanism of QSOX1 secretion in the epididymis.

doi:10.6342/NTU201903813

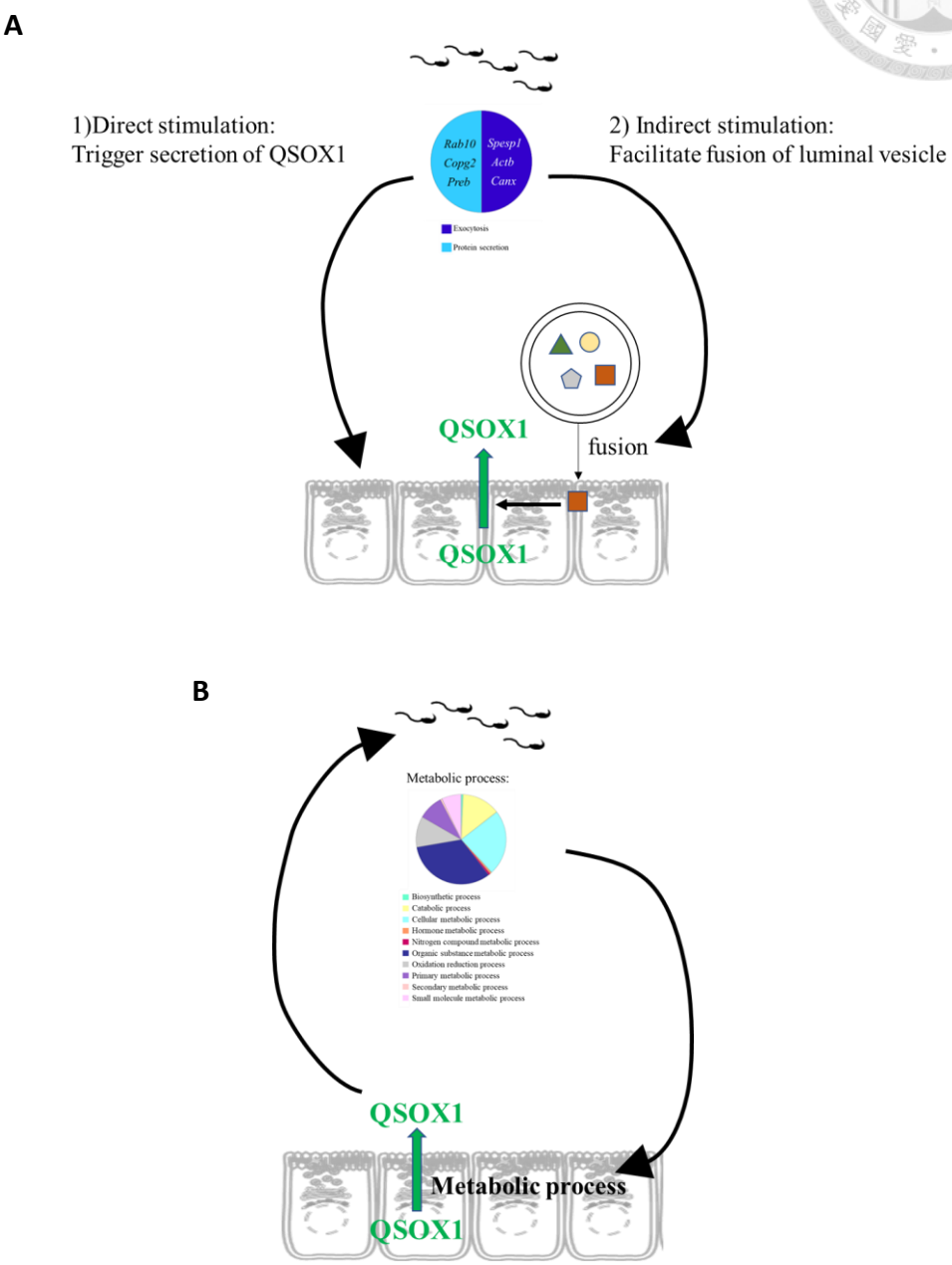

Figure 17. Predicted regulatory pathway of QSOX1 secretion in the epididymis.

(A) The relationship of the QSOX1 secretion and those proteins participated in exocytosis and membrane fusion process. (B) The relationship of the QSOX1 secretion and the enzyme release from sperm.

doi:10.6342/NTU201903813

Reference

[1] W.C. YOUNG, A Study of the Function of the Epididymis: III. Functional Changes Undergone by Spermatozoa During Their Passage Through the Epididymis and Vas Deferens in the Guinea-Pig, Journal of Experimental Biology 8(2) (1931) 151-162.
[2] J. Bedford, Effects of duct ligation on the fertilzing ability of spermatozoa from different regions of the rabbit epididymis, Journal of Experimental Zoology 166(2) (1967) 271-281.
[3] M. Orgebin-Crist, Sperm maturation in rabbit epididymis, Nature 216(5117) (1967) 816.
[4] J. Martan, Epididymal histochemistry and physiology, Biology of reproduction 1(suppl_1) (1969) 134-154.
[5] W.W. Shum, N. Da Silva, D. Brown, S. Breton, Regulation of luminal acidification in the male reproductive tract via cell–cell crosstalk, Journal of Experimental Biology 212(11) (2009) 1753-1761.
[6] J.-L. Dacheux, S. Castella, J.L. Gatti, F. Dacheux, Epididymal cell secretory activities and the role of proteins in boar sperm maturation, Theriogenology 63(2) (2005) 319-341.
[7] M. Gregory, D.G. Cyr, The blood-epididymis barrier and inflammation, Spermatogenesis 4(2) (2014) e979619.
[8] J.-L. Dacheux, F. Dacheux, New insights into epididymal function in relation to sperm maturation, Reproduction 147(2) (2014) R27-R42.
[9] B. Nixon, G.N. De Iuliis, H.M. Hart, W. Zhou, A. Mathe, I.R. Bernstein, A.L. Anderson, S.J. Stanger, D.A. Skerrett-Byrne, M.F.B. Jamaluddin, Proteomic profiling of mouse epididymosomes reveals their contributions to post-testicular sperm maturation, Molecular & Cellular Proteomics 18(Supplement 1) (2019) S91-S108.
[10] A. Akintayo, C. Légaré, R. Sullivan, Dicarbonyl L-xylulose reductase (DCXR), a "moonlighting protein" in the bovine epididymis, PloS one 10(3) (2015) e0120869-e0120869.
[11] H.I. Calvin, J.M. Bedford, Formation of disulphide bonds in the nucleus and accessory structures of mammalian spermatozoa during maturation in the epididymis, J Reprod Fertil Suppl 13 (1971) Suppl 13:65-75.
[12] R. Shalgi, J. Seligman, N.S. Kosower, Dynamics of the thiol status of rat spermatozoa during maturation: analysis with the fluorescent labeling agent monobromobimane, Biol Reprod 40(5) (1989) 1037-45.

doi:10.6342/NTU201903813

[13] H. Moore, Contribution of epididymal factors to sperm maturation and storage, Andrologia 30(4-5) (1998) 233-239.
[14] J. Bedford, The maturation of spermatozoa in the human epididymis, J Reprod Fertil (supple) 18 (1973) 199-213.
[15] M.E. Cabrillana, M. de los Ángeles Monclus, T.E.S. Lancellotti, P.V. Boarelli, A.E. Vincenti, M.M. Fornés, E.A. Sanabria, M.W. Fornés, Thiols of flagellar proteins are essential for progressive motility in human spermatozoa, Reproduction, Fertility and Development 29(7) (2017) 1435-1446.
[16] C. Jeulin, L.M. Lewin, C. Chevrier, D. Schoevaert-Brossault, Changes in flagellar movement of rat spermatozoa along the length of the epididymis: Manual and computer-aided image analysis, Cell motility and the cytoskeleton 35(2) (1996) 147-161.
[17] L. Hetherington, E.K. Schneider, C. Scott, D. DeKretser, C.H. Muller, H. Hondermarck, T. Velkov, M.A. Baker, Deficiency in Outer Dense Fiber 1 is a marker and potential driver of idiopathic male infertility, Molecular & Cellular Proteomics 15(12) (2016) 3685-3693.
[18] D. Evenson, L. Jost, D. Marshall, M. Zinaman, E. Clegg, K. Purvis, P. De Angelis, O. Claussen, Utility of the sperm chromatin structure assay as a diagnostic and prognostic tool in the human fertility clinic, Human reproduction 14(4) (1999) 1039-1049.
[19] H.I. Calvin, C.C. Yu, J.M. Bedford, Effects of epididymal maturation, zinc (II) and copper (II) on the reactive sulfhydryl content of structural elements in rat spermatozoa, Exp Cell Res 81(2) (1973) 333-41.
[20] J.M. Hutchison, D.C. Rau, J.E. DeRouchey, Role of Disulfide Bonds on DNA Packaging Forces in Bull Sperm Chromatin, Biophys J 113(9) (2017) 1925-1933.
[21] R. Balhorn, The protamine family of sperm nuclear proteins, Genome biology 8(9) (2007) 227.
[22] M.A. Szczygiel, W.S. Ward, Combination of dithiothreitol and detergent treatment of spermatozoa causes paternal chromosomal damage, Biology of reproduction 67(5) (2002) 1532-1537.
[23] J. Bedford, H. Calvin, Changes in S S linked structures of the sperm tail during epididymal maturation, with comparative observations in sub-mammalian species, Journal of Experimental Zoology 187(2) (1974) 181-203.
[24] B. Benayoun, A. Esnard-Fève, S. Castella, Y. Courty, F. Esnard, Rat Seminal Vesicle FAD-dependent Sulfhydryl Oxidase BIOCHEMICAL CHARACTERIZATION AND MOLECULAR CLONING OF A MEMBER OF THE NEW SULFHYDRYL OXIDASE/QUIESCIN Q6 GENE FAMILY, Journal of Biological Chemistry 276(17) (2001) 13830-13837.

doi:10.6342/NTU201903813

[25] T. Chang, B.R. Zirkin, Distribution of sulfhydryl oxidase activity in the rat and hamster male reproductive tract, Biology of reproduction 18(5) (1978) 745-748.
[26] M.C. Ostrowski, W. Kistler, Properties of a flavoprotein sulfhydryl oxidase from rat seminal vesicle secretion, Biochemistry 19(12) (1980) 2639-2645.
[27] D.L. Coppock, C. Kopman, S. Scandalis, S. Gilleran, Preferential gene expression in quiescent human lung fibroblasts, Cell growth and differentiation 4 (1993) 483-483.
[28] I. Grossman, A. Alon, T. Ilani, D. Fass, An inhibitory antibody blocks the first step in the dithiol/disulfide relay mechanism of the enzyme QSOX1, Journal of molecular biology 425(22) (2013) 4366-4378.
[29] C. Thorpe, K.L. Hoober, S. Raje, N.M. Glynn, J. Burnside, G.K. Turi, D.L. Coppock, Sulfhydryl oxidases: emerging catalysts of protein disulfide bond formation in eukaryotes, Archives of biochemistry and biophysics 405(1) (2002) 1-12.
[30] J.-F. Musard, M. Sallot, P. Dulieu, A. Fraîchard, C. Ordener, J.-P. Remy-Martin, M. Jouvenot, P. Adami, Identification and expression of a new sulfhydryl oxidase SOx-3 during the cell cycle and the estrus cycle in uterine cells, Biochemical and biophysical research communications 287(1) (2001) 83-91.
[31] A. Tury, G. Mairet-Coello, F. Poncet, C. Jacquemard, P. Risold, D. Fellmann, B. Griffond, QSOX sulfhydryl oxidase in rat adenohypophysis: localization and regulation by estrogens, Journal of endocrinology 183(2) (2004) 353-363.
[32] G. Mairet-Coello, A. Tury, A. Esnard-Feve, D. Fellmann, P.Y. Risold, B. Griffond, FAD-linked sulfhydryl oxidase QSOX: Topographic, cellular, and subcellular immunolocalization in adult rat central nervous system, Journal of Comparative Neurology 473(3) (2004) 334-363.
[33] D. Coppock, C. Kopman, J. Gudas, D.A. Cina-Poppe, Regulation of the quiescence-induced genes: quiescin Q6, decorin, and ribosomal protein S29, Biochemical and biophysical research communications 269(2) (2000) 604-610.
[34] S. Chakravarthi, C.E. Jessop, M. Willer, C.J. Stirling, N.J. Bulleid, Intracellular catalysis of disulfide bond formation by the human sulfhydryl oxidase, QSOX1, Biochemical Journal 404(3) (2007) 403-411.
[35] T.-E. Wang, S.-H. Li, S. Minabe, A.L. Anderson, M.D. Dun, K.-I. Maeda, F. Matsuda, H.-W. Chang, B. Nixon, P.-S.J. Tsai, Mouse quiescin sulfhydryl oxidases exhibit distinct epididymal luminal distribution with segment-specific sperm surface associations, Biology of reproduction 99(5) (2018) 1022-1033.
[36] T. Chang, B. Morton, Epididymal sulfhydryl oxidase: a sperm-protective enzyme from the male reproductive tract, Biochemical and biophysical research communications 66(1) (1975) 309-315.

doi:10.6342/NTU201903813

[37] B. Hinton, Z. Lan, D. Rudolph, J. Labus, R. Lye, Testicular regulation of epididymal gene expression, Journal of reproduction and fertility. Supplement 53 (1998) 47-57.
[38] X. Liu, F. Liu, In-depth mapping of human testicular and epididymal proteins and their functional association with spermatozoa, Molecular medicine reports 12(1) (2015) 173-179.
[39] J.-L. Gatti, X. Druart, Y. Guérin, F. Dacheux, J.-L. Dacheux, A 105-to 94-kilodalton protein in the epididymal fluids of domestic mammals is angiotensin I-converting enzyme (ACE); evidence that sperm are the source of this ACE, Biology of reproduction 60(4) (1999) 937-945.
[40] E. Casillas, P. Villalobos, R. Gonzales, Distribution of carnitine and acylcarnitine in the hamster epididymis and in epididymal spermatozoa during maturation, Reproduction 72(1) (1984) 197-201.
[41] L. Hermo, B. Robaire, The epididymis from molecular to clinical practice. A comprehensive survey of the efferent ducts, the epididymis and the vas deferens, Epididymal cell types and their functions. New York: Kluwer Academic/Plenum Publishers (2002) 81-102.
[42] A.P. Hoffer, D.W. Hamilton, D.W. Fawcett, The ultrastructure of the principal cells and intraepithelial leucocytes in the initial segment of the rat epididymis, The Anatomical Record 175(2) (1973) 169-201.
[43] B. Robaire, L. Hermo, Efferent ducts, epididymis, and vas deferens: structure, functions, and their regulation, The physiology of reproduction 1 (1988) 999-1080.
[44] L. Nicander, Comparative studies on the fine structure of vertebrate spermatozoa, Academic Press, New York (1970) 47-56.
[45] L. Nicander, T. Glover, Regional histology and fine structue of the epididymal duct in the golden hamster (Mesocricetus auratus), Journal of anatomy 114(Pt 3) (1973) 347.
[46] L. Nicander, M. Malmqvist, Ultrastructural observations suggesting merocrine secretion in the initial segment of the mammalian epididymis, Cell and tissue research 184(4) (1977) 487-490.
[47] R.B. Kelly, Pathways of protein secretion in eukaryotes, Science 230(4721) (1985) 25-32.
[48] M. Steinhoff, W. Eicheler, P. Holterhus, U. Rausch, J. Seitz, G. Aumüller, Hormonally induced changes in apocrine secretion of transglutaminase in the rat dorsal prostate and coagulating gland, European journal of cell biology 65(1) (1994) 49-59.

doi:10.6342/NTU201903813

[49] Y. AGRAWAL, T. VANHA-PERTTULA, Electron microscopic study of the secretion process in bovine reproductive organs, Journal of andrology 9(5) (1988) 307-316.
[50] L. HERMO, H.I. ADAMALI, S. ANDONIAN, Immunolocalization of CA II and H+ V-ATPase in epithelial cells of the mouse and rat epididymis, Journal of andrology 21(3) (2000) 376-391.
[51] H.O. Goyal, Morphology of the bovine epididymis, American Journal of Anatomy 172(2) (1985) 155-172.
[52] B.T.H. Bernard Robaire, 2 and Marie-Claire Orgebin-Crist3, Chapter22 The epididymis, 2006.
[53] D. Brooks, Epididymal functions and their hormonal regulation, Australian journal of biological sciences 36(3) (1983) 205-222.
[54] S. Sujarit, R. Jones, B. Setchell, G. Chaturapanich, M. Lin, J. Clulow, Stimulation of protein secretion in the initial segment of the rat epididymis by fluid from the ram rete testis, Reproduction 88(1) (1990) 315-321.
[55] J.T.M. Vreeburg, DISTRIBUTION OF TESTOSTERONE AND 5α-DIHYDRO-TESTOSTERONE IN RAT EPIDIDYMIS AND THEIR CONCENTRATIONS IN EFFERENT DUCT FLUID, Journal of Endocrinology 67(2) (1975) 203-210.
[56] N. Ezer, B. Robaire, Androgenic regulation of the structure and functions of the epididymis, The epididymis: from molecules to clinical practice, Springer2002, pp. 297-316.
[57] D. Brooks, Effect of androgens on protein synthesis and secretion in various regions of the rat epididymis, as analysed by two-dimensional gel electrophoresis, Molecular and cellular endocrinology 29(3) (1983) 255-270.
[58] E. Castellon, C. Huidobro, Androgen regulation of glycosidase secretion in epithelial cell cultures from human epididymis, Human Reproduction 14(6) (1999) 1522-1527.
[59] R. Jones, C. Brown, K. Von Glos, M. Parker, Hormonal regulation of protein synthesis in the rat epididymis. Characterization of androgen-dependent and testicular fluid-dependent proteins, Biochemical Journal 188(3) (1980) 667-676.
[60] J.E. Garrett, S.H. Garrett, J. Douglass, A spermatozoa-associated factor regulates proenkephalin gene expression in the rat epididymis, Molecular Endocrinology 4(1) (1990) 108-118.
[61] C. Reyes-Moreno, J. Laflamme, G. Frenette, M.A. Sirard, R. Sullivan, Spermatozoa modulate epididymal cell proliferation and protein secretion in vitro, Molecular Reproduction and Development: Incorporating Gamete Research 75(3) (2008) 512-520.

doi:10.6342/NTU201903813

[62] S. Skerget, M.A. Rosenow, K. Petritis, T.L. Karr, Sperm proteome maturation in the mouse epididymis, PLoS One 10(11) (2015) e0140650.
[63] A.-J. Liang, G.-S. Wang, P. Ping, S.-G. Hu, Y. Lin, Y. Ma, Z.-Z. Duan, H.-S. Wang, F. Sun, The expression of the new epididymal luminal protein of PDZ domain containing 1 is decreased in asthenozoospermia, Asian journal of andrology 20(2) (2018) 154.
[64] G. Bindea, B. Mlecnik, H. Hackl, P. Charoentong, M. Tosolini, A. Kirilovsky, W.-H. Fridman, F. Pagès, Z. Trajanoski, J. Galon, ClueGO: a Cytoscape plug-in to decipher functionally grouped gene ontology and pathway annotation networks, Bioinformatics 25(8) (2009) 1091-1093.
[65] E.A. Castellón, C.C. Huidobro, Androgen regulation of glycosidase secretion in epithelial cell cultures from human epididymis, Human Reproduction 14(6) (1999) 1522-1527.
[66] T.G. Cooper, The epididymis, sperm maturation and fertilisation, Springer Science & Business Media2012.
[67] R. Shabanowitz, G. Killian, Two-dimensional electrophoresis of proteins in principal cells, spermatozoa, and fluid associated with the rat epididymis, Biology of reproduction 36(3) (1987) 753-768.
[68] C.J. Flickinger, Regional differences in synthesis, intracellular transport, and secretion of protein in the mouse epididymis, Biology of reproduction 25(4) (1981) 871-883.
[69] J. Dacheux, F. Dacheux, M. Paquignon, Changes in sperm surface membrane and luminal protein fluid content during epididymal transit in the boar, Biology of reproduction 40(3) (1989) 635-651.
[70] P. Ross, F.W. Kan, P. Antaki, N. Vigneault, A. Chapdelaine, K.D. Roberts, Protein synthesis and secretion in the human epididymis and immunoreactivity with sperm antibodies, Molecular reproduction and development 26(1) (1990) 12-23.
[71] B.T. Hinton, M.A. Palladino, Epididymal epithelium: its contribution to the formation of a luminal fluid microenvironment, Microscopy research and technique 30(1) (1995) 67-81.
[72] P. Syntin, J.-L. Dacheux, F.o. Dacheux, Postnatal development and regulation of proteins secreted in the boar epididymis, Biology of reproduction 61(6) (1999) 1622-1635.
[73] A. Abou-Haila, M. Fain-Maurel, Postnatal differentiation of the enzymatic activity of the mouse epididymis, International journal of andrology 8(6) (1985) 441-458.
[74] H. Ueda, T. Hirano, S. Fujimoto, Changes in protein secretory patterns during the development of the rat epididymis, Zoological science 7(4) (1990) p681-690.

doi:10.6342/NTU201903813

[75] M. Orgebin-Crist, B. Danzo, J. Davies, Endocrine control of the development and maintenance of sperm fertilizing ability in the epididymis, (1975).
[76] D. Brooks, Metabolic activity in the epididymis and its regulation by androgens, Physiological reviews 61(3) (1981) 515-555.
[77] M.K. HOLLAND, J.T. VREEBURG, M.C. ORGEBIN-CRIST, Testicular regulation of epididymal protein secretion, Journal of andrology 13(3) (1992) 266-273.
[78] C. Jean-Faucher, M. Berger, M. de Turckheim, G. Veyssiere, C. Jean, Testosterone and dihydrotestosterone levels in the epididymis, vas deferens and preputial gland of mice during sexual maturation, International journal of andrology 8(1) (1985) 44-57.
[79] B. Robaire, M. Hamzeh, Androgen action in the epididymis, Journal of andrology 32(6) (2011) 592-599.
[80] M. Bendahmane, A. Abou-Haila, Synthesis, characterization and hormonal regulation of epididymal proteins during postnatal development of the mouse, Differentiation 55(2) (1994) 119-125.
[81] F.C. Janca, L.K. Jost, D.P. Evenson, Mouse testicular and sperm cell development characterized from birth to adulthood by dual parameter flow cytometry, Biology of reproduction 34(4) (1986) 613-623.
[82] P. Sipilä, R. Shariatmadari, I.T. Huhtaniemi, M. Poutanen, Immortalization of epididymal epithelium in transgenic mice expressing simian virus 40 T antigen: characterization of cell lines and regulation of the polyoma enhancer activator 3, Endocrinology 145(1) (2004) 437-446.
[83] Y. ARAKI, K. SUZUKI, R.J. MATUSIK, M. OBINATA, M.C. ORGEBIN-CRIST, Immortalized epididymal cell lines from transgenic mice overexpressing temperature-sensitive simian virus 40 large T-antigen gene, Journal of andrology 23(6) (2002) 854-869.
[84] P. Seiler, T.G. Cooper, E. Nieschlag, Sperm number and condition affect the number of basal cells and their expression of macrophage antigen in the murine epididymis, International journal of andrology 23(2) (2000) 65-76.
[85] J.E. Ellington, D.P. Evenson, J.E. Fleming, R.S. Brisbois, G.A. Hiss, S.J. Broder, R.W. Wright Jr, Coculture of human sperm with bovine oviduct epithelial cells decreases sperm chromatin structural changes seen during culture in media alone, Fertility and sterility 69(4) (1998) 643-649.
[86] R.-C. Chian, M.-A. Sirard, Fertilizing ability of bovine spermatozoa cocultured with oviduct epithelial cells, Biology of reproduction 52(1) (1995) 156-162.

doi:10.6342/NTU201903813

[87] M.E. Kervancioglu, E. Saridogan, R.J. Aitken, O. Djahanbakhch, Importance of sperm-to-epithelial cell contact for the capacitation of human spermatozoa in fallopian tube epithelial cell cocultures, Fertility and sterility 74(4) (2000) 780-784.
[88] A.E. Elweza, M.A. Ezz, T.J. Acosta, A.K. Talukder, T. Shimizu, H. Hayakawa, M. Shimada, K. Imakawa, A.H. Zaghloul, A. Miyamoto, A proinflammatory response of bovine endometrial epithelial cells to active sperm in vitro, Molecular reproduction and development 85(3) (2018) 215-226.
[89] G.R. Klinefelter, A novel system for the co-culture of epididymal epithelial cells and sperm from adult rats, Journal of tissue culture methods 14(4) (1992) 195-200.
[90] M. Yeste, W.V. Holt, S. Bonet, J.E. Rodríguez-Gil, R.E. Lloyd, Viable and morphologically normal boar spermatozoa alter the expression of heat-shock protein genes in oviductal epithelial cells during co-culture in vitro, Molecular reproduction and development 81(9) (2014) 805-819.
[91] N. Saraswathy, P. Ramalingam, 10 - Introduction to proteomics, in: N. Saraswathy, P. Ramalingam (Eds.), Concepts and Techniques in Genomics and Proteomics, Woodhead Publishing2011, pp. 147-158.
[92] T.E. Angel, U.K. Aryal, S.M. Hengel, E.S. Baker, R.T. Kelly, E.W. Robinson, R.D. Smith, Mass spectrometry-based proteomics: existing capabilities and future directions, Chemical Society Reviews 41(10) (2012) 3912-3928.
[93] E.R. Wasbrough, S. Dorus, S. Hester, J. Howard-Murkin, K. Lilley, E. Wilkin, A. Polpitiya, K. Petritis, T.L. Karr, The Drosophila melanogaster sperm proteome-II (DmSP-II), Journal of proteomics 73(11) (2010) 2171-2185.

doi:10.6342/NTU201903813

Table 1. List of caput sperm origin protein IDs in sperm epithelium co-culture medium

Family	Member	Database	Accession	uniprot id	Score	Mass	Num. of matche s	Num. of significant matches	Num. of significant sequences	Num. of significant sequences	emPAI	Description
4	2	NCBIprot	ACTB_MOUSE		1886	39161	85	85	20	20	22.18	prot. beta-actin (aa 27-375), partial [Mus musculus]
9	1	SwissProt	LDHC_MOUSE	Ldhc	1757	35889	71	71	22	22	23.41	L-lactate dehydrogenase C chain OS=Mus musculus OX=10090 GN=Ldhc PE=1 SV=2
15	1	NCBIprot	AATM_MOUSE	Got2	1504	47382	72	72	29	29	18.35	aspartate aminotransferase precursor [Mus musculus]
28	1	SwissProt	KIC18_MOUSE	Krt18	1186	47509	40	40	25	25	9.27	Keratin, type I cytoskeletal 18 OS=Mus musculus OX=10090 GN=Krt18 PE=1 SV=5
32	1	SwissProt	GLNA_MOUSE	Glul	1000	42092	48	48	17	17	9.21	Glutamine synthetase OS=Mus musculus OX=10090 GN=Glul PE=1 SV=6
36	1	SwissProt	LMNB1_MOUSE	Lmnb1	873	66719	44	44	36	36	10.37	lamin B [Mus musculus]
17	2	NCBIprot	ALDH2_MOUSE	Aldh2	815	56502	36	36	21	21	4.26	Aldehyde dehydrogenase, mitochondrial OS=Mus musculus OX=10090 GN=Aldh2 PE=1 SV=1
48	1	SwissProt	HSP72_MOUSE	Hspa2	813	69599	35	35	21	21	2.63	Heat shock-related 70 kDa protein 2 OS=Mus musculus OX=10090 GN=Hspa2 PE=1 SV=2
1	3	SwissProt	Q7M739_MOUSE	Tpr	790	266764	29	29	28	28	0.57	TPA: cstp: nuclear pore complex-associated intranuclear coiled-coil protein TPR [Mus musculus]
51	1	NCBIprot	ALI4A1_MOUSE	Eif4a1a1	762	54433	32	32	22	22	5.06	Retinal dehydrogenase 1 OS=Mus musculus OX=10090 GN=Aldh1a1 PE=1 SV=5
48	2	SwissProt	KIC2L_MOUSE	Krt8	744	54531	39	39	26	26	7.93	Keratin, type II cytoskeletal 8 OS=Mus musculus OX=10090 GN=Krt8 PE=1 SV=4
24	5	SwissProt	HYOU1_MOUSE	Hyou1	647	111112	28	28	19	19	1.24	Hypoxia up-regulated protein 1 OS=Mus musculus OX=10090 GN=Hyou1 PE=1 SV=1
67	1	SwissProt	HNRPK_MOUSE	Hnrnpk	625	50944	29	29	17	17	3.14	Heterogeneous nuclear ribonucleoprotein K OS=Mus musculus OX=10090 GN=Hnrnpk PE=1 SV=1
73	1	SwissProt	ALBU_MOUSE	Alb	623	68648	24	24	19	19	2.26	Serum albumin OS=Mus musculus OX=10090 GN=Alb PE=1 SV=3
32	7	SwissProt	TBA3_MOUSE	Tuba3a	622	49928	24	24	14	14	2.59	Tubulin alpha-3 chain OS=Mus musculus OX=10090 GN=Tuba3a PE=1 SV=1
1	4	SwissProt	HS71L_MOUSE	Hspa1l	611	70593	25	25	14	14	1.33	Heat shock 70 kDa protein 1-like OS=Mus musculus OX=10090 GN=Hspa1l PE=1 SV=4
82	1	NCBIprot	Q8OUW7_MOUSE	Iqgap1	569	188652	25	25	23	23	0.69	IQ motif containing GTPase activating protein 1 [Mus musculus]
28	2	SwissProt	KIC19_MOUSE	Krt19	555	44515	24	24	18	18	5.14	Keratin, type I cytoskeletal 19 OS=Mus musculus OX=10090 GN=Krt19 PE=1 SV=1
104	1	SwissProt	ZPBP1_MOUSE	Zpbp	511	39206	21	21	11	11	2.29	Zona pellucida-binding protein 1 OS=Mus musculus OX=10090 GN=Zpbp PE=1 SV=2
119	1	SwissProt	PYR1_MOUSE	Cad	475	243084	17	17	13	13	0.26	CAD protein OS=Mus musculus OX=10090 GN=Cad PE=1 SV=1
126	1	SwissProt	ODO1_MOUSE	Oqdh	458	116375	21	18	18	18	0.94	2-oxoglutarate dehydrogenase, mitochondrial OS=Mus musculus OX=10090 GN=Oqdh PE=1 SV=3
141	1	SwissProt	SUOX_MOUSE	Suox	454	60718	19	19	15	15	1.87	Sulfite oxidase, mitochondrial OS=Mus musculus OX=10090 GN=Suox PE=1 SV=2
134	2	SwissProt	GSTM7_MOUSE	Gstm7	422	25963	18	18	12	12	6.21	Glutathione S-transferase Mu 7 OS=Mus musculus OX=10090 GN=Gstm7 PE=1 SV=1
142	1	SwissProt	MMSA_MOUSE	Aldh6a1	418	57878	18	18	15	15	2.02	Methylmalonate-semialdehyde dehydrogenase [acylating], mitochondrial OS=Mus musculus OX=10090 GN=Aldh6a1 PE=1 SV=1
144	1	SwissProt	LDHD_MOUSE	Ldhd	417	51815	16	16	13	13	1.91	Probable D-lactate dehydrogenase, mitochondrial OS=Mus musculus OX=10090 GN=Ldhd PE=1 SV=1
155	1	NCBIprot	Q83255_MOUSE	Ctnnb1	404	85416	17	17	16	16	1.23	Catenin beta-1 OS=Mus musculus OX=10090 GN=Ctnnb1 PE=1 SV=1
156	1	NCBIprot	Q83255_MOUSE	Naglu	404	82544	14	14	13	13	0.96	alpha-N-acetylglucosaminidase precursor [Mus musculus]
24	7	SwissProt	KC1C7_MOUSE	Krt7	396	50678	17	17	15	15	2.52	Keratin, type II cytoskeletal 7 OS=Mus musculus OX=10090 GN=Krt7 PE=1 SV=1
162	1	SwissProt	HZAT5_MOUSE	Hzaf5	395	39710	16	16	12	12	2.61	Core histone macro-H2A.1 OS=Mus musculus OX=10090 GN=H2afy PE=1 SV=3
169	1	NCBIprot	Q6PAC1_MOUSE	Gsn	387	80712	15	15	13	13	0.99	gelsolin isoform 2 [Mus musculus]
179	1	SwissProt	SACA1_MOUSE	Spaca1	375	33321	12	12	6	6	1.77	Sperm acrosome membrane-associated protein 1 OS=Mus musculus OX=10090 GN=Spaca1 PE=1 SV=1
195	1	SwissProt	NUCB2_MOUSE	Nucb2	357	50273	21	21	18	18	4	Nucleobindin-2 OS=Mus musculus OX=10090 GN=Nucb2 PE=1 SV=2
196	1	SwissProt	THIM_MOUSE	Acaa2	356	41803	15	15	14	14	3.14	3-ketoacyl-CoA thiolase, mitochondrial OS=Mus musculus OX=10090 GN=Acaa2 PE=1 SV=3
124	2	SwissProt	PLSL_MOUSE	Lcp1	351	70105	18	18	18	18	1.99	Plastin-2 OS=Mus musculus OX=10090 GN=Lcp1 PE=1 SV=4
203	1	SwissProt	AT2A2_MOUSE	Atp2a2	346	114784	15	15	11	11	0.56	Sarcoplasmic/endoplasmic reticulum calcium ATPase 2 OS=Mus musculus OX=10090 GN=Atp2a2 PE=1 SV=2
215	1	SwissProt	CTNA1_MOUSE	Ctnna1	331	100044	13	13	11	11	0.6	Catenin alpha-1 OS=Mus musculus OX=10090 GN=Ctnna1 PE=1 SV=1
219	1	SwissProt	RS8_MOUSE	Rps8	327	24190	17	17	12	12	7.1	40S ribosomal protein S8 OS=Mus musculus OX=10090 GN=Rps8 PE=1 SV=2
221	1	SwissProt	MTHAP_MOUSE	Spata18	324	60360	11	7	7	7	0.89	Mitochondrion-eating protein OS=Mus musculus OX=10090 GN=Spata18 PE=2 SV=2
223	1	SwissProt	ENPP5_MOUSE	Enpp5	322	54552	14	14	11	11	1.56	Ectonucleotide pyrophosphatase/phosphodiesterase family member 5 OS=Mus musculus OX=10090 GN=Enpp5 PE=1 SV=3
206	3	SwissProt	PP1G_MOUSE	Ppp1c	318	36960	14	14	11	11	2.54	Serine/threonine-protein phosphatase PP1-gamma catalytic subunit OS=Mus musculus OX=10090 GN=Ppp1c PE=1 SV=1
235	1	SwissProt	SDHA_MOUSE	Sdha	307	72539	10	8	8	8	0.6	Succinate dehydrogenase [ubiquinone] flavoprotein subunit, mitochondrial OS=Mus musculus OX=10090 GN=Sdha PE=1 SV=1
243	1	SwissProt	ADAM7_MOUSE	Adam7	301	89129	16	16	14	14	0.96	Disintegrin and metalloproteinase domain-containing protein 7 OS=Mus musculus OX=10090 GN=Adam7 PE=2 SV=2
246	1	SwissProt	ECHP1_MOUSE	Ech1	261	124195	11	11	11	11	0.58	Angiotensin-converting enzyme OS=Mus musculus OX=10090 GN=Ace PE=1 SV=3
249	1	SwissProt	DJC10_MOUSE	Dnajc10	296	90225	12	12	12	12	0.76	Dnaj homolog subfamily C member 10 OS=Mus musculus OX=10090 GN=Dnajc10 PE=1 SV=2
261	1	SwissProt	RS2_MOUSE	Rps2	284	31212	19	19	12	12	5.69	40S ribosomal protein S2 OS=Mus musculus OX=10090 GN=Rps2 PE=1 SV=3
279	1	SwissProt	LCN2_MOUSE	Lcn2	272	21000	7	7	6	6	2.33	Epididymal-specific lipocalin-5 OS=Mus musculus OX=10090 GN=Lcn5 PE=1 SV=1
280	1	NCBIprot	Q8BVP2_MOUSE	Ldha6b	272	42022	7	7	5	5	0.66	L-lactate dehydrogenase A-like 6B [Mus musculus]
284	1	SwissProt	PGRC1_MOUSE	Pgrmc1	271	21681	9	9	6	6	2.21	Membrane-associated progesterone receptor component 1 OS=Mus musculus OX=10090 GN=Pgrmc1 PE=1 SV=4
205	2	NCBIprot	CALX_MOUSE	Cmax	268	64971	15	15	10	10	0.93	calnexin, partial [Mus musculus domesticus]
11	2	SwissProt	EPIPL_MOUSE	Epdr1	261	72419 5	11	11	11	11	0.07	Epiplakin OS=Mus musculus OX=10090 GN=Epdr1 PE=1 SV=2
134	5	SwissProt	GSTM1_MOUSE	Gstm1	260	25953	10	10	6	6	2.12	Glutathione S-transferase Mu 1 OS=Mus musculus OX=10090 GN=Gstm1 PE=1 SV=2
295	1	SwissProt	RPN2_MOUSE	Rpn2	238	69020	9	9	8	8	0.64	Dolichyl-diphosphooligosaccharide--protein glycosyltransferase subunit 2 OS=Mus musculus OX=10090 GN=Rpn2 PE=1 SV=1
299	1	SwissProt	RL3_MOUSE	Rpl3	234	46081	11	7	7	7	1.52	60S ribosomal protein L3 OS=Mus musculus OX=10090 GN=Rpl3 PE=1 SV=3
303	1	SwissProt	MIC60_MOUSE	Immt	232	83848	11	9	9	9	0.58	MICOS complex subunit Mic60 OS=Mus musculus OX=10090 GN=Immt PE=1 SV=1
315	1	SwissProt	FABP9_MOUSE	Fabp9	247	15008	7	6	6	6	4.31	Fatty acid-binding protein 9 OS=Mus musculus OX=10090 GN=Fabp9 PE=1 SV=2
134	8	SwissProt	GSTM5_MOUSE	Gstm5	246	26617	15	15	13	13	8.21	Glutathione S-transferase Mu 5 OS=Mus musculus OX=10090 GN=Gstm5 PE=1 SV=1
320	1	SwissProt	EPCAM_MOUSE	Epcam	243	34996	8	8	6	6	1.07	Epithelial cell adhesion molecule OS=Mus musculus OX=10090 GN=Epcam PE=1 SV=1
321	1	SwissProt	CAPZB_MOUSE	Capzb	243	31326	4	4	4	4	0.72	F-actin-capping protein subunit beta OS=Mus musculus OX=10090 GN=Capzb PE=1 SV=3
324	1	SwissProt	NLTP_MOUSE	Scp2	242	59088	11	8	8	8	0.78	Non-specific lipid-transfer protein OS=Mus musculus OX=10090 GN=Scp2 PE=1 SV=3

doi:10.6342/NTU201903813

325	1	SwissProt	CLUS_MOUSE	Clu	241	51623	13	13	8	8	0.93	Clusterin OS=Mus musculus OX=10090 GN=Clu PE=1 SV=1
326	2	NCBIprot	SODM_MOUSE	Sod2	236	24619	10	10	5	5	1.35	manganese superoxide dismutase [Mus musculus]
341	1	SwissProt	RPN1_MOUSE	Rpn1	228	68486	10	10	6	6	0.45	Dolichyl-diphosphooligosaccharide--protein glycosyltransferase subunit 1 OS=Mus musculus OX=10090 GN=Rpn1 PE=1 SV=1
355	1	SwissProt	MA2B2_MOUSE	Man2b2	222	115537	10	10	9	9	0.4	Epididymis-specific alpha-mannosidase OS=Mus musculus OX=10090 GN=Man2b2 PE=1 SV=2
364	1	SwissProt	ECH1_MOUSE	Ech1	216	36095	6	6	6	6	1.03	Delta(3,5)-Delta(2,4)-dienoyl-CoA isomerase, mitochondrial OS=Mus musculus OX=10090 GN=Ech1 PE=1 SV=1
381	1	SwissProt	GOGA5_MOUSE	Golga5	211	82318	8	8	8	8	0.51	Golgin subfamily A member 5 OS=Mus musculus OX=10090 GN=Golga5 PE=1 SV=2
400	1	SwissProt	ACRO_MOUSE	Acr	204	48898	6	6	6	6	0.68	Acrosin OS=Mus musculus OX=10090 GN=Acr PE=1 SV=1
148	4	SwissProt	ERP44_MOUSE	Erp44	203	46823	12	12	9	9	1.26	Endoplasmic reticulum resident protein 44 OS=Mus musculus OX=10090 GN=Erp44 PE=1 SV=1
407	1	NCBIprot	Q8K1M3_MOUSE	Prkar2a	200	45561	9	9	7	7	0.92	cAMP-dependent protein kinase type II-alpha regulatory subunit [Mus musculus]
415	1	SwissProt	LMAN2_MOUSE	Lman2	195	40404	6	6	6	6	0.88	Vesicular integral-membrane protein VIP36 OS=Mus musculus OX=10090 GN=Lman2 PE=1 SV=2
430	1	SwissProt	SPESP_MOUSE	Spesp1	191	44674	10	10	10	10	1.59	Sperm equatorial segment protein 1 OS=Mus musculus OX=10090 GN=Spesp1 PE=1 SV=2
432	1	SwissProt	PPT1_MOUSE	Ppt1	191	34467	11	11	7	7	1.36	Palmitoyl-protein thioesterase 1 OS=Mus musculus OX=10090 GN=Ppt1 PE=1 SV=2
433	1	SwissProt	ODPB_MOUSE	Pdhb	190	38912	8	8	6	6	0.92	Pyruvate dehydrogenase E1 component subunit beta, mitochondrial OS=Mus musculus OX=10090 GN=Pdhb PE=1 SV=1
463	1	SwissProt	CACP_MOUSE	Crat	181	70794	8	8	8	8	0.62	Carnitine O-acetyltransferase OS=Mus musculus OX=10090 GN=Crat PE=1 SV=3
330	2	SwissProt	ARF5_MOUSE	Arf5	178	20517	7	7	5	5	1.78	ADP-ribosylation factor 5 OS=Mus musculus OX=10090 GN=Arf5 PE=1 SV=2
492	1	SwissProt	HEXB_MOUSE	Hexb	171	61077	10	10	10	10	1.01	Beta-hexosaminidase subunit beta OS=Mus musculus OX=10090 GN=Hexb PE=1 SV=2
497	1	SwissProt	CD166_MOUSE	Alcam	169	65051	7	7	7	7	0.58	CD166 antigen OS=Mus musculus OX=10090 GN=Alcam PE=1 SV=3
500	1	SwissProt	IPYR2_MOUSE	Ppa2	169	38090	6	6	5	5	0.75	Inorganic pyrophosphatase 2, mitochondrial OS=Mus musculus OX=10090 GN=Ppa2 PE=1 SV=1
291	3	SwissProt	CISY_MOUSE	Cs	160	51703	6	6	5	5	0.51	Citrate synthase, mitochondrial OS=Mus musculus OX=10090 GN=Cs PE=1 SV=1
528	1	SwissProt	THIL_MOUSE	Acat1	159	44787	7	7	7	7	0.95	Acetyl-CoA acetyltransferase, mitochondrial OS=Mus musculus OX=10090 GN=Acat1 PE=1 SV=1
533	1	SwissProt	MIC19_MOUSE	Chchd3	158	26318	3	3	3	3	0.62	MICOS complex subunit Mic19 OS=Mus musculus OX=10090 GN=Chchd3 PE=1 SV=1
534	1	SwissProt	RCN1_MOUSE	Rcn1	158	38090	8	8	8	8	1.44	Reticulocalbin-1 OS=Mus musculus OX=10090 GN=Rcn1 PE=1 SV=1
535	1	SwissProt	LMAN1_MOUSE	Lman1	157	57753	5	5	4	4	0.34	Protein ERGIC-53 OS=Mus musculus OX=10090 GN=Lman1 PE=1 SV=1
537	1	SwissProt	GBB1_MOUSE	Gnb1	157	37353	6	6	5	5	0.76	Guanine nucleotide-binding protein G(I)/G(S)/G(T) subunit beta-1 OS=Mus musculus OX=10090 GN=Gnb1 PE=1 SV=3
251	2	SwissProt	SC23A_MOUSE	Sec23a	156	86106	7	7	6	6	0.35	Protein transport protein Sec23A OS=Mus musculus OX=10090 GN=Sec23a PE=1 SV=2
542	1	SwissProt	DPEP3_MOUSE	Dpep3	155	54213	8	8	7	7	0.73	Dipeptidase 3 OS=Mus musculus OX=10090 GN=Dpep3 PE=1 SV=1
545	1	SwissProt	ROP1_MOUSE	Ropn1	155	23987	7	7	5	5	1.87	Ropporin-1 OS=Mus musculus OX=10090 GN=Ropn1 PE=1 SV=1
100	4	SwissProt	HBB2_MOUSE	Hbb-b2	153	15868	6	6	5	5	2.73	Hemoglobin subunit beta-2 OS=Mus musculus OX=10090 GN=Hbb-b2 PE=1 SV=2
34	2	SwissProt	MYH10_MOUSE	Myh10	151	228855	3	3	3	3	0.06	Myosin-10 OS=Mus musculus OX=10090 GN=Myh10 PE=1 SV=2
559	1	SwissProt	TOM22_MOUSE	Tomm22	150	15527	3	3	3	3	1.24	Mitochondrial import receptor subunit TOM22 homolog OS=Mus musculus OX=10090 GN=Tomm22 PE=1 SV=3
562	1	SwissProt	TMF1_MOUSE	Tmf1	150	121729	5	5	3	3	0.11	TATA element modulatory factor OS=Mus musculus OX=10090 GN=Tmf1 PE=1 SV=2
560	1	SwissProt	AT1A1_MOUSE	Atp1a1	149	112910	5	5	5	5	0.21	Sodium/potassium-transporting ATPase subunit alpha-1 OS=Mus musculus OX=10090 GN=Atp1a1 PE=1 SV=1
578	1	SwissProt	KAD3_MOUSE	Ak3	146	25410	6	6	6	6	1.71	GTP:AMP phosphotransferase AK3, mitochondrial OS=Mus musculus OX=10090 GN=Ak3 PE=1 SV=3
579	1	SwissProt	BGAL_MOUSE	Glb1	146	73074	4	4	4	4	0.26	Beta-galactosidase OS=Mus musculus OX=10090 GN=Glb1 PE=1 SV=1
575	1	NCBIprot	B2RWH8_MOUSE	Gm4846	146	61604	4	4	2	2	0.15	flavin-containing monooxygenase 13 [Mus musculus]
585	1	NCBIprot	GCSH_MOUSE	Gcsh	144	18577	4	4	3	3	0.97	Gcsh protein [Mus musculus]
293	2	SwissProt	RAB1B_MOUSE	Rab1b	142	22173	5	5	4	4	1.14	Ras-related protein Rab-1B OS=Mus musculus OX=10090 GN=Rab1b PE=1 SV=1
605	1	SwissProt	HIBCH_MOUSE	Hibch	137	43010	6	6	6	6	0.81	3-hydroxyisobutyryl-CoA hydrolase, mitochondrial OS=Mus musculus OX=10090 GN=Hibch PE=1 SV=1
608	1	SwissProt	CLPP_MOUSE	Clpp	136	29781	5	5	3	3	0.53	ATP-dependent Clp protease proteolytic subunit, mitochondrial OS=Mus musculus OX=10090 GN=Clpp PE=1 SV=1
616	1	SwissProt	ODP2_MOUSE	Dlat	134	67899	4	4	4	4	0.29	Dihydrolipoyllysine-residue acetyltransferase component of pyruvate dehydrogenase complex, mitochondrial OS=Mus musculus OX=10090 GN=Dlat PE=1 SV=2
619	1	SwissProt	RL13_MOUSE	Rpl13	133	24290	5	5	5	5	1.38	60S ribosomal protein L13 OS=Mus musculus OX=10090 GN=Rpl13 PE=1 SV=3
621	1	SwissProt	ASGL1_MOUSE	Asrgl1	133	33928	5	5	5	5	0.87	Isoaspartyl peptidase/L-asparaginase OS=Mus musculus OX=10090 GN=Asrgl1 PE=1 SV=1
625	1	SwissProt	ECHM_MOUSE	Echs1	131	31454	5	5	3	3	0.5	Enoyl-CoA hydratase, mitochondrial OS=Mus musculus OX=10090 GN=Echs1 PE=1 SV=1
626	1	SwissProt	3HIDH_MOUSE	Hibadh	131	35417	6	6	4	4	0.61	3-hydroxyisobutyrate dehydrogenase, mitochondrial OS=Mus musculus OX=10090 GN=Hibadh PE=1 SV=1
628	1	SwissProt	LYPD4_MOUSE	Lypd4	131	26979	3	3	3	3	0.6	Ly6/PLAUR domain-containing protein 4 OS=Mus musculus OX=10090 GN=Lypd4 PE=1 SV=1
631	1	SwissProt	FAHD1_MOUSE	Fahd1	130	25156	3	3	3	3	0.65	Acylpyruvase FAHD1, mitochondrial OS=Mus musculus OX=10090 GN=Fahd1 PE=1 SV=2
641	1	SwissProt	ACOT2_MOUSE	Acot2	128	49626	5	5	4	4	0.41	Acyl-coenzyme A thioesterase 2, mitochondrial OS=Mus musculus OX=10090 GN=Acot2 PE=1 SV=2
648	1	SwissProt	A1AT1_MOUSE	Serpina1s	126	45974	3	3	3	3	0.32	Alpha-1-antitrypsin 1-1 OS=Mus musculus OX=10090 GN=Serpina1a PE=1 SV=4
659	1	NCBIprot	B9PWQ7_MOUSE	Zan	124	584262	9	9	9	9	0.07	zonadhesin precursor [Mus musculus]
661	1	SwissProt	H10_MOUSE	H1f0	123	20848	3	3	2	2	0.5	Histone H1.0 OS=Mus musculus OX=10090 GN=H1f0 PE=2 SV=4
377	2	SwissProt	AT2B4_MOUSE	Atp2b4	122	132984	4	4	4	4	0.14	Plasma membrane calcium-transporting ATPase 4 OS=Mus musculus OX=10090 GN=Atp2b4 PE=1 SV=1
667	1	SwissProt	SYTL4_MOUSE	Sytl4	122	75974	4	4	4	4	0.25	Synaptotagmin-like protein 4 OS=Mus musculus OX=10090 GN=Sytl4 PE=1 SV=1
670	1	SwissProt	G6PE_MOUSE	H6pd	122	88872	3	3	3	3	0.16	GDH/6PGL endoplasmic bifunctional protein OS=Mus musculus OX=10090 GN=H6pd PE=1 SV=2
690	1	SwissProt	LBTM1_MOUSE	Letm1	119	82937	5	5	4	4	0.23	Mitochondrial proton/calcium exchanger protein OS=Mus musculus OX=10090 GN=Letm1 PE=1 SV=1
698	1	SwissProt	NSF_MOUSE	Nsf	117	82561	7	7	7	7	0.44	Vesicle-fusing ATPase OS=Mus musculus OX=10090 GN=Nsf PE=1 SV=2
718	1	SwissProt	GPRL1_MOUSE	Glipr1l1	114	27057	3	3	3	3	0.6	GLIPR1-like protein 1 OS=Mus musculus OX=10090 GN=Glipr1l1 PE=1 SV=1
726	1	SwissProt	ISC2A_MOUSE	Isoc2a	113	22403	4	4	4	4	1.12	Isochorismatase domain-containing protein 2A OS=Mus musculus OX=10090 GN=Isoc2a PE=1 SV=1
742	1	SwissProt	ETFB_MOUSE	Etfb	109	27606	4	4	4	4	0.84	Electron transfer flavoprotein subunit beta OS=Mus musculus OX=10090 GN=Etfb PE=1 SV=3
750	1	SwissProt	NHLC3_MOUSE	Nhlrc3	108	38171	3	3	3	3	0.4	NHL repeat-containing protein 3 OS=Mus musculus OX=10090 GN=Nhlrc3 PE=1 SV=1
377	3	SwissProt	AT2B1_MOUSE	Atp2b1	107	134662	4	4	4	4	0.14	Plasma membrane calcium-transporting ATPase 1 OS=Mus musculus OX=10090 GN=Atp2b1 PE=1 SV=1
755	1	SwissProt	TM9S2_MOUSE	Tm9sf2	107	75280	6	6	5	5	0.33	Transmembrane 9 superfamily member 2 OS=Mus musculus OX=10090 GN=Tm9sf2 PE=1 SV=1
768	1	SwissProt	HPDL_MOUSE	Hpdl	104	39884	4	4	4	4	0.53	4-hydroxyphenylpyruvate dioxygenase-like protein OS=Mus musculus OX=10090 GN=Hpdl PE=2 SV=1
770	1	SwissProt	SUCB1_MOUSE	Sucla2	104	50082	5	5	5	5	0.53	Succinate--CoA ligase [ADP-forming] subunit beta, mitochondrial OS=Mus musculus OX=10090 GN=Sucla2 PE=1 SV=2
777	1	SwissProt	FSCB_MOUSE	Fscb	103	114909	4	4	4	4	0.16	Fibrous sheath CABYR-binding protein OS=Mus musculus OX=10090 GN=Fscb PE=1 SV=1

doi:10.6342/NTU201903813

781	1	SwissProt	GSTK1_MOUSE	Gstk1	103	25687	3	3	3	3	0.64	Glutathione S-transferase kappa 1 OS=Mus musculus OX=10090 GN=Gstk1 PE=1 SV=3
786	1	SwissProt	CUZD1_MOUSE	Cuzd1	102	68038	5	5	5	5	0.37	CUB and zona pellucida-like domain-containing protein 1 OS=Mus musculus OX=10090 GN=Cuzd1 PE=1 SV=2
139	3	SwissProt	COPG2_MOUSE	Copg2	101	97617	4	4	4	4	0.19	Coatomer subunit gamma-2 OS=Mus musculus OX=10090 GN=Copg2 PE=1 SV=1
795	1	SwissProt	TMED3_MOUSE	Tmed3	101	25449	2	2	2	2	0.39	Transmembrane emp24 domain-containing protein 3 OS=Mus musculus OX=10090 GN=Tmed3 PE=1 SV=1
798	1	SwissProt	CBR1_MOUSE	Cbr1	100	30622	5	5	5	5	1	Carbonyl reductase [NADPH] 1 OS=Mus musculus OX=10090 GN=Cbr1 PE=1 SV=3
802	1	SwissProt	FA71B_MOUSE	Fam71b	100	68842	3	3	3	3	0.2	Protein FAM71B OS=Mus musculus OX=10090 GN=Fam71b PE=3 SV=3
805	1	SwissProt	SRPRB_MOUSE	Srprb	99	29561	4	4	4	4	0.77	Signal recognition particle receptor subunit beta OS=Mus musculus OX=10090 GN=Srprb PE=1 SV=1
811	1	SwissProt	SDHB_MOUSE	Sdhb	97	31793	3	3	3	3	0.49	Succinate dehydrogenase [ubiquinone] iron-sulfur subunit, mitochondrial OS=Mus musculus OX=10090 GN=Sdhb PE=1 SV=1
812	1	SwissProt	ABHDA_MOUSE	Abhd10	97	33019	3	3	3	3	0.47	Mycophenolic acid acyl-glucuronide esterase, mitochondrial OS=Mus musculus OX=10090 GN=Abhd10 PE=1 SV=1
817	1	SwissProt	GTR3_MOUSE	Slc2a3	97	53444	2	2	1	1	0.17	Solute carrier family 2, facilitated glucose transporter member 3 OS=Mus musculus OX=10090 GN=Slc2a3 PE=1 SV=1
819	1	SwissProt	BPHL_MOUSE	Bphl	97	32830	4	4	4	4	0.68	Valacyclovir hydrolase OS=Mus musculus OX=10090 GN=Bphl PE=1 SV=1
822	1	SwissProt	TX101_MOUSE	Tex101	97	26980	3	3	3	3	0.6	Testis-expressed protein 101 OS=Mus musculus OX=10090 GN=Tex101 PE=1 SV=1
826	1	SwissProt	ECHA_MOUSE	Hadha	96	82617	3	3	3	3	0.17	Trifunctional enzyme subunit alpha, mitochondrial OS=Mus musculus OX=10090 GN=Hadha PE=1 SV=1
837	1	SwissProt	NDUV2_MOUSE	Ndufv2	94	27268	5	5	4	4	0.86	NADH dehydrogenase [ubiquinone] flavoprotein 2, mitochondrial OS=Mus musculus OX=10090 GN=Ndufv2 PE=1 SV=2
838	1	SwissProt	HDHD3_MOUSE	Hdhd3	94	28009	5	5	4	4	0.83	Haloacid dehalogenase-like hydrolase domain-containing protein 3 OS=Mus musculus OX=10090 GN=Hdhd3 PE=1 SV=1
849	1	NCBIprot	GCP60_MOUSE	Acbd3	93	60144	3	3	2	2	0.15	RecName: Full=Golgi resident protein GCP60; AltName: Full=Acyl-CoA-binding domain-containing protein 3; AltName: Full=Golgi complex-associated protein 1; Short=GOCAP1; AltName: Full=Golgi phosphoprotein 1; Short=GOLPH1; AltName: F
857	1	SwissProt	TMX1_MOUSE	Tmx1	92	31376	3	3	2	2	0.31	Thioredoxin-related transmembrane protein 1 OS=Mus musculus OX=10090 GN=Tmx1 PE=1 SV=1
856	1	NCBIprot	Q30KN1_MOUSE	Defb47	92	8834	2	2	2	2	1.51	beta-defensin 130-like precursor [Mus musculus]
862	1	SwissProt	DBLOH_MOUSE	Diablo	91	26804	3	3	3	3	0.61	Diablo homolog, mitochondrial OS=Mus musculus OX=10090 GN=Diablo PE=1 SV=2
24	11	SwissProt	K2C71_MOUSE	Krt71	90	57347	3	3	3	3	0.25	Keratin, type II cytoskeletal 71 OS=Mus musculus OX=10090 GN=Krt71 PE=1 SV=1
867	1	SwissProt	RL18A_MOUSE	Rpl18a	90	20719	3	3	3	3	0.84	60S ribosomal protein L18a OS=Mus musculus OX=10090 GN=Rpl18a PE=1 SV=1
876	1	NCBIprot	Q0VDQ2_MOUSE	Gykl1	89	59864	2	2	2	2	0.15	Glycerol kinase-like 1 [Mus musculus]
541	2	SwissProt	RAB5B_MOUSE	Rab5b	88	23692	3	3	3	3	0.71	Ras-related protein Rab-5B OS=Mus musculus OX=10090 GN=Rab5b PE=1 SV=1
882	1	SwissProt	CYB5B_MOUSE	Cyb5b	88	16308	2	2	2	2	0.67	Cytochrome b5 type B OS=Mus musculus OX=10090 GN=Cyb5b PE=1 SV=1
886	1	SwissProt	RL32_MOUSE	Rpl32	88	15850	4	4	3	3	1.2	60S ribosomal protein L32 OS=Mus musculus OX=10090 GN=Rpl32 PE=1 SV=2
890	1	SwissProt	TXD12_MOUSE	Txndc12	87	19036	4	4	4	4	1.42	Thioredoxin domain-containing protein 12 OS=Mus musculus OX=10090 GN=Txndc12 PE=1 SV=1
892	1	SwissProt	MIC27_MOUSE	Apool	86	29242	3	3	3	3	0.54	MICOS complex subunit Mic27 OS=Mus musculus OX=10090 GN=Apool PE=1 SV=1
900	1	SwissProt	CATC_MOUSE	Ctsc	86	52343	3	3	3	3	0.28	Dipeptidyl peptidase 1 OS=Mus musculus OX=10090 GN=Ctsc PE=1 SV=1
800	2	SwissProt	VAPB_MOUSE	Vapb	84	26929	3	3	2	2	0.37	Vesicle-associated membrane protein-associated protein B OS=Mus musculus OX=10090 GN=Vapb PE=1 SV=3
910	1	SwissProt	VAMP3_MOUSE	Vamp3	84	11473	1	1	1	1	0.44	Vesicle-associated membrane protein 3 OS=Mus musculus OX=10090 GN=Vamp3 PE=1 SV=1
912	1	SwissProt	SSDH_MOUSE	Aldh5a1	84	55933	3	3	3	3	0.26	Succinate-semialdehyde dehydrogenase, mitochondrial OS=Mus musculus OX=10090 GN=Aldh5a1 PE=1 SV=1
923	1	SwissProt	MVP_MOUSE	Mvp	83	95865	4	4	4	4	0.2	Major vault protein OS=Mus musculus OX=10090 GN=Mvp PE=1 SV=4
933	1	NCBIprot	BPNT1_MOUSE	Bpnt1	81	33222	6	6	5	5	0.89	Bisphosphate 3'-nucleotidase 1 [Mus musculus]
945	1	SwissProt	ABD12_MOUSE	Abhd12	80	45241	1	1	1	1	0.1	Monoacylglycerol lipase ABHD12 OS=Mus musculus OX=10090 GN=Abhd12 PE=1 SV=2
952	1	SwissProt	NDUA8_MOUSE	Ndufa8	79	19979	3	3	3	3	0.88	NADH dehydrogenase [ubiquinone] 1 alpha subcomplex subunit 8 OS=Mus musculus OX=10090 GN=Ndufa8 PE=1 SV=3
977	1	SwissProt	ODPAT_MOUSE	Pdha2	77	43385	2	2	2	2	0.22	Pyruvate dehydrogenase E1 component subunit alpha, testis-specific form, mitochondrial OS=Mus musculus OX=10090 GN=Pdha2 PE=1 SV=1
992	1	SwissProt	KBL_MOUSE	Gcat	75	44902	2	2	2	2	0.21	2-amino-3-ketobutyrate coenzyme A ligase, mitochondrial OS=Mus musculus OX=10090 GN=Gcat PE=1 SV=2
993	1	SwissProt	TIM50_MOUSE	Timm50	75	39752	2	2	2	2	0.24	Mitochondrial import inner membrane translocase subunit TIM50 OS=Mus musculus OX=10090 GN=Timm50 PE=1 SV=1
1006	1	SwissProt	ACSL1_MOUSE	Acsl1	74	77901	2	2	2	2	0.12	Long-chain-fatty-acid--CoA ligase 1 OS=Mus musculus OX=10090 GN=Acsl1 PE=1 SV=2
1007	1	SwissProt	EST5A_MOUSE	Ces5a	74	64126	2	2	2	2	0.14	Carboxylesterase 5A OS=Mus musculus OX=10090 GN=Ces5a PE=2 SV=1
1017	1	SwissProt	NSDHL_MOUSE	Nsdhl	73	40660	3	3	3	3	0.37	Sterol-4-alpha-carboxylate 3-dehydrogenase, decarboxylating OS=Mus musculus OX=10090 GN=Nsdhl PE=1 SV=1
1018	1	SwissProt	ERAP1_MOUSE	Erap1	73	106531	2	2	2	2	0.08	Endoplasmic reticulum aminopeptidase 1 OS=Mus musculus OX=10090 GN=Erap1 PE=1 SV=2
1021	1	SwissProt	TIM16_MOUSE	Pam16	73	13776	1	1	1	1	0.35	Mitochondrial import inner membrane translocase subunit TIM16 OS=Mus musculus OX=10090 GN=Pam16 PE=1 SV=1
1025	1	SwissProt	MACD1_MOUSE	Macrod1	73	35272	2	2	2	2	0.27	ADP-ribose glycohydrolase MACROD1 OS=Mus musculus OX=10090 GN=Macrod1 PE=1 SV=2
1029	1	SwissProt	SIAT1_MOUSE	St6gal1	72	46556	3	3	3	3	0.32	Beta-galactoside alpha-2,6-sialyltransferase 1 OS=Mus musculus OX=10090 GN=St6gal1 PE=1 SV=2
1030	1	SwissProt	THEM4_MOUSE	Them4	72	26015	2	2	2	2	0.38	Acyl-coenzyme A thioesterase THEM4 OS=Mus musculus OX=10090 GN=Them4 PE=1 SV=1
1035	1	SwissProt	AMRP_MOUSE	Lrpap1	71	42189	3	3	3	3	0.35	Alpha-2-macroglobulin receptor-associated protein OS=Mus musculus OX=10090 GN=Lrpap1 PE=1 SV=1
1037	1	SwissProt	PREB_MOUSE	Preb	71	45409	1	1	1	1	0.1	Prolactin regulatory element-binding protein OS=Mus musculus OX=10090 GN=Preb PE=1 SV=1
1038	1	SwissProt	CLPT1_MOUSE	Clptm1	71	75243	2	2	2	2	0.12	Cleft lip and palate transmembrane protein 1 homolog OS=Mus musculus OX=10090 GN=Clptm1 PE=1 SV=1
1041	1	SwissProt	QSOX2_MOUSE	Qsox2	70	77726	3	3	3	3	0.18	Sulfhydryl oxidase 2 OS=Mus musculus OX=10090 GN=Qsox2 PE=1 SV=1
1051	1	SwissProt	PPIF_MOUSE	Ppif	69	21723	1	1	1	1	0.21	Peptidyl-prolyl cis-trans isomerase F, mitochondrial OS=Mus musculus OX=10090 GN=Ppif PE=1 SV=1
1053	1	SwissProt	NDUS5_MOUSE	Ndufs5	69	12639	2	2	2	2	0.93	NADH dehydrogenase [ubiquinone] iron-sulfur protein 5 OS=Mus musculus OX=10090 GN=Ndufs5 PE=1 SV=3
1058	1	SwissProt	GALNS_MOUSE	Galns	69	57637	4	4	4	4	0.34	N-acetylgalactosamine-6-sulfatase OS=Mus musculus OX=10090 GN=Galns PE=1 SV=2
1074	1	SwissProt	RL8_MOUSE	Rpl8	67	28007	2	2	2	2	0.35	60S ribosomal protein L8 OS=Mus musculus OX=10090 GN=Rpl8 PE=1 SV=2
1075	1	SwissProt	IAH1_MOUSE	Iah1	67	27956	3	3	3	3	0.57	Isoamyl acetate-hydrolyzing esterase 1 homolog OS=Mus musculus OX=10090 GN=Iah1 PE=1 SV=1
1081	1	SwissProt	APOA1_MOUSE	Apoa1	66	30597	3	3	3	3	0.51	Apolipoprotein A-I OS=Mus musculus OX=10090 GN=Apoa1 PE=1 SV=2
1083	1	SwissProt	OCAD1_MOUSE	Ociad1	66	27593	1	1	1	1	0.17	OCIA domain-containing protein 1 OS=Mus musculus OX=10090 GN=Ociad1 PE=1 SV=1
1094	1	SwissProt	DFB20_MOUSE	Defb20	65	11032	3	3	3	3	2.09	Beta-defensin 20 OS=Mus musculus OX=10090 GN=Defb20 PE=3 SV=1
1097	1	SwissProt	ITM2B_MOUSE	Itm2b	65	30240	3	3	2	2	0.32	Integral membrane protein 2B OS=Mus musculus OX=10090 GN=Itm2b PE=1 SV=1
1100	1	SwissProt	ARGI2_MOUSE	Arg2	65	38854	3	3	3	3	0.39	Arginase-2, mitochondrial OS=Mus musculus OX=10090 GN=Arg2 PE=1 SV=1
1109	1	SwissProt	PREP_MOUSE	Pitrm1	64	117297	3	3	3	3	0.12	Presequence protease, mitochondrial OS=Mus musculus OX=10090 GN=Pitrm1 PE=1 SV=1
1111	1	SwissProt	DNJC3_MOUSE	Dnajc3	64	57428	1	1	1	1	0.08	DnaJ homolog subfamily C member 3 OS=Mus musculus OX=10090 GN=Dnajc3 PE=1 SV=1
1085	1	SwissProt	HEXA_MOUSE	Hexa	63	60574	2	2	2	2	0.15	Beta-hexosaminidase subunit alpha OS=Mus musculus OX=10090 GN=Hexa PE=1 SV=2
1114	1	SwissProt	CABYR_MOUSE	Cabyr	63	48303	3	3	3	3	0.3	Calcium-binding tyrosine phosphorylation-regulated protein OS=Mus musculus OX=10090 GN=Cabyr PE=1 SV=1

doi:10.6342/NTU201903813

1117	1	NCBIprot	Q9Z2P7_MOUSE	Vti1b	63	26465	2	2	2	2	0.38	GES30 [Mus musculus]
1116	1	NCBIprot	DGUOK_MOUSE	Dguok	63	32202	1	1	1	1	0.14	deoxyguanosine kinase 1 [Mus musculus]
1122	1	SwissProt	PLBL2_MOUSE	Plbd2	62	66247	4	4	4	4	0.29	Putative phospholipase B-like 2 OS=Mus musculus OX=10090 GN=Plbd2 PE=1 SV=2
1131	1	SwissProt	GPDA_MOUSE	Gpd1	62	37548	3	3	3	3	0.4	Glycerol-3-phosphate dehydrogenase [NAD(+)], cytoplasmic OS=Mus musculus OX=10090 GN=Gpd1 PE=1 SV=3
1142	1	SwissProt	PCCA_MOUSE	Pcca	61	79871	1	1	1	1	0.05	Propionyl-CoA carboxylase alpha chain, mitochondrial OS=Mus musculus OX=10090 GN=Pcca PE=1 SV=2
1154	1	SwissProt	PCCB_MOUSE	Pccb	60	58372	2	2	2	2	0.16	Propionyl-CoA carboxylase beta chain, mitochondrial OS=Mus musculus OX=10090 GN=Pccb PE=1 SV=2
1150	1	NCBIprot	Q91WP8_MOUSE	Ndufv3	60	50494	1	1	1	1	0.09	NADH dehydrogenase (ubiquinone) flavoprotein 3 [Mus musculus]
1172	1	SwissProt	LAT1_MOUSE	Slc7a5	59	55836	2	2	1	1	0.08	Large neutral amino acids transporter small subunit 1 OS=Mus musculus OX=10090 GN=Slc7a5 PE=1 SV=2
1174	1	SwissProt	BCAT2_MOUSE	Bcat2	58	44099	1	1	1	1	0.1	Branched-chain-amino-acid aminotransferase, mitochondrial OS=Mus musculus OX=10090 GN=Bcat2 PE=1 SV=2
1182	1	SwissProt	GALT2_MOUSE	Galnt2	57	64473	2	2	2	2	0.14	Polypeptide N-acetylgalactosaminyltransferase 2 OS=Mus musculus OX=10090 GN=Galnt2 PE=1 SV=1
1191	1	SwissProt	ENPP1_MOUSE	Enpp1	57	103109	3	3	3	3	0.13	Ectonucleotide pyrophosphatase/phosphodiesterase family member 1 OS=Mus musculus OX=10090 GN=Enpp1 PE=1 SV=4
1194	1	SwissProt	NDUS4_MOUSE	Ndufs4	57	19772	2	2	1	1	0.24	NADH dehydrogenase [ubiquinone] iron-sulfur protein 4, mitochondrial OS=Mus musculus OX=10090 GN=Ndufs4 PE=1 SV=3
1185	1	NCBIprot	CC136_MOUSE	Ccdc136	57	35870	1	1	1	1	0.13	RecName: Full=BTB/POZ domain-containing protein KCTD12; AltName: Full=Pfetin; AltName: Full=Predominantly fetal expressed T1 domain
1198	1	SwissProt	GCC2_MOUSE	Gcc2	56	194325	1	1	1	1	0.02	GRIP and coiled-coil domain-containing protein 2 OS=Mus musculus OX=10090 GN=Gcc2 PE=1 SV=2
1201	1	SwissProt	NDUA2_MOUSE	Ndufa2	56	10909	1	1	1	1	0.46	NADH dehydrogenase [ubiquinone] 1 alpha subcomplex subunit 2 OS=Mus musculus OX=10090 GN=Ndufa2 PE=1 SV=3
1160	1	SwissProt	MCCB_MOUSE	Mccc2	55	61340	2	2	2	2	0.15	Methylcrotonoyl-CoA carboxylase beta chain, mitochondrial OS=Mus musculus OX=10090 GN=Mccc2 PE=1 SV=1
1205	1	SwissProt	ESYT1_MOUSE	Esyt1	55	121478	2	2	2	2	0.07	Extended synaptotagmin-1 OS=Mus musculus OX=10090 GN=Esyt1 PE=1 SV=2
1208	1	SwissProt	TPP1_MOUSE	Tpp1	55	61304	3	3	3	3	0.23	Tripeptidyl-peptidase 1 OS=Mus musculus OX=10090 GN=Tpp1 PE=1 SV=2
1213	1	SwissProt	FAF2_MOUSE	Faf2	54	52438	1	1	1	1	0.08	FAS-associated factor 2 OS=Mus musculus OX=10090 GN=Faf2 PE=1 SV=2
1222	1	SwissProt	TMX3_MOUSE	Tmx3	54	51815	1	1	1	1	0.09	Protein disulfide-isomerase TMX3 OS=Mus musculus OX=10090 GN=Tmx3 PE=1 SV=2
876	3	SwissProt	GLPK2_MOUSE	Gk2	53	60590	2	2	2	2	0.15	Glycerol kinase 2 OS=Mus musculus OX=10090 GN=Gk2 PE=1 SV=1
1233	1	SwissProt	DHRS4_MOUSE	Dhrs4	53	29866	1	1	1	1	0.15	Dehydrogenase/reductase SDR family member 4 OS=Mus musculus OX=10090 GN=Dhrs4 PE=1 SV=3
1244	1	SwissProt	COQ9_MOUSE	Coq9	52	35061	1	1	1	1	0.13	Ubiquinone biosynthesis protein COQ9, mitochondrial OS=Mus musculus OX=10090 GN=Coq9 PE=1 SV=1
1245	1	SwissProt	SDF2L_MOUSE	Sdf2l1	52	23634	2	2	2	2	0.43	Stromal cell-derived factor 2-like protein 1 OS=Mus musculus OX=10090 GN=Sdf2l1 PE=1 SV=2
1255	1	SwissProt	PPBT_MOUSE	Alpl	52	57478	2	2	2	2	0.16	Alkaline phosphatase, tissue-nonspecific isozyme OS=Mus musculus OX=10090 GN=Alpl PE=1 SV=2
1256	1	SwissProt	ADA28_MOUSE	Adam28	51	88612	2	2	2	2	0.1	Disintegrin and metalloproteinase domain-containing protein 28 OS=Mus musculus OX=10090 GN=Adam28 PE=1 SV=3
1264	1	SwissProt	BAP31_MOUSE	Bcap31	51	27939	1	1	1	1	0.16	B-cell receptor-associated protein 31 OS=Mus musculus OX=10090 GN=Bcap31 PE=1 SV=4
1273	1	SwissProt	BASI_MOUSE	Bsg	50	42418	2	2	1	1	0.11	Basigin OS=Mus musculus OX=10090 GN=Bsg PE=1 SV=2
1274	1	NCBIprot	Q80VE6_MOUSE	Nup205	50	48521	1	1	1	1	0.09	Nup205 protein, partial [Mus musculus]
1290	1	SwissProt	ADT4_MOUSE	Slc25a31	49	35235	1	1	1	1	0.13	ADP/ATP translocase 4 OS=Mus musculus OX=10090 GN=Slc25a31 PE=1 SV=1
1292	1	SwissProt	LCN8_MOUSE	Lcn8	49	19853	2	2	2	2	0.53	Epididymal-specific lipocalin-8 OS=Mus musculus OX=10090 GN=Lcn8 PE=2 SV=1
1291	1	NCBIprot	SCAM2_MOUSE	Scamp2	49	41154	1	1	1	1	0.11	PREDICTED: secretory carrier-associated membrane protein 2 isoform X1 [Mus musculus]
1302	1	SwissProt	FIS1_MOUSE	Fis1	48	16998	3	3	3	3	1.09	Mitochondrial fission 1 protein OS=Mus musculus OX=10090 GN=Fis1 PE=1 SV=1
1304	1	SwissProt	DYSF_MOUSE	Dysf	48	237759	1	1	1	1	0.02	Dysferlin OS=Mus musculus OX=10090 GN=Dysf PE=1 SV=3
1306	1	SwissProt	NB5R3_MOUSE	Cyb5r3	48	34106	2	2	2	2	0.28	NADH-cytochrome b5 reductase 3 OS=Mus musculus OX=10090 GN=Cyb5r3 PE=1 SV=3
1337	1	SwissProt	DJB11_MOUSE	Dnajb11	46	40530	3	3	2	2	0.23	DnaJ homolog subfamily B member 11 OS=Mus musculus OX=10090 GN=Dnajb11 PE=1 SV=1
1345	1	SwissProt	IVD_MOUSE	Ivd	46	46296	1	1	1	1	0.1	Isovaleryl-CoA dehydrogenase, mitochondrial OS=Mus musculus OX=10090 GN=Ivd PE=1 SV=1
1355	1	SwissProt	NDUS8_MOUSE	Ndufs8	45	24023	1	1	1	1	0.19	NADH dehydrogenase [ubiquinone] iron-sulfur protein 8, mitochondrial OS=Mus musculus OX=10090 GN=Ndufs8 PE=1 SV=1
1360	1	SwissProt	NDUB4_MOUSE	Ndufb4	45	15072	1	1	1	1	0.32	NADH dehydrogenase [ubiquinone] 1 beta subcomplex subunit 4 OS=Mus musculus OX=10090 GN=Ndufb4 PE=1 SV=3
1365	1	SwissProt	RAB18_MOUSE	Rab18	45	23021	2	2	2	2	0.44	Ras-related protein Rab-18 OS=Mus musculus OX=10090 GN=Rab18 PE=1 SV=2
1371	1	SwissProt	DBIL5_MOUSE	Dbil5	44	9858	3	3	2	2	1.3	Diazepam-binding inhibitor-like 5 OS=Mus musculus OX=10090 GN=Dbil5 PE=1 SV=1
1378	1	SwissProt	5NT1B_MOUSE	Nt5c1b	44	64962	1	1	1	1	0.07	Cytosolic 5'-nucleotidase 1B OS=Mus musculus OX=10090 GN=Nt5c1b PE=2 SV=2
1386	1	SwissProt	OST48_MOUSE	Ddost	44	48997	1	1	1	1	0.09	Dolichyl-diphosphooligosaccharide--protein glycosyltransferase 48 kDa subunit OS=Mus musculus OX=10090 GN=Ddost PE=1 SV=2
1388	1	SwissProt	P5CR2_MOUSE	Pycr2	44	33638	2	2	2	2	0.29	Pyrroline-5-carboxylate reductase 2 OS=Mus musculus OX=10090 GN=Pycr2 PE=1 SV=1
1397	1	SwissProt	HPCL1_MOUSE	Hpcal1	43	22324	1	1	1	1	0.21	Hippocalcin-like protein 1 OS=Mus musculus OX=10090 GN=Hpcal1 PE=1 SV=2
1433	1	SwissProt	MPPA_MOUSE	Pmpca	42	58242	1	1	1	1	0.08	Mitochondrial-processing peptidase subunit alpha OS=Mus musculus OX=10090 GN=Pmpca PE=1 SV=1
1435	1	SwissProt	IQGA2_MOUSE	Iqgap2	42	180416	1	1	1	1	0.02	Ras GTPase-activating-like protein IQGAP2 OS=Mus musculus OX=10090 GN=Iqgap2 PE=1 SV=2
1438	1	SwissProt	GPD1L_MOUSE	Gpd1l	41	38201	1	1	1	1	0.12	Glycerol-3-phosphate dehydrogenase 1-like protein OS=Mus musculus OX=10090 GN=Gpd1l PE=1 SV=2
1439	1	SwissProt	ZFPL1_MOUSE	Zfpl1	41	34133	1	1	1	1	0.13	Zinc finger protein-like 1 OS=Mus musculus OX=10090 GN=Zfpl1 PE=1 SV=1
1445	1	SwissProt	LYRIC_MOUSE	Mtdh	41	63808	2	2	2	2	0.14	Protein LYRIC OS=Mus musculus OX=10090 GN=Mtdh PE=1 SV=1
1446	1	SwissProt	ECHB_MOUSE	Hadhb	41	51353	1	1	1	1	0.09	Trifunctional enzyme subunit beta, mitochondrial OS=Mus musculus OX=10090 GN=Hadhb PE=1 SV=1
1449	1	SwissProt	HINT2_MOUSE	Hint2	41	17309	1	1	1	1	0.27	Histidine triad nucleotide-binding protein 2, mitochondrial OS=Mus musculus OX=10090 GN=Hint2 PE=1 SV=1
1456	1	SwissProt	TMED4_MOUSE	Tmed4	40	26005	2	2	2	2	0.38	Transmembrane emp24 domain-containing protein 4 OS=Mus musculus OX=10090 GN=Tmed4 PE=1 SV=1
1462	1	SwissProt	NAGAB_MOUSE	Naga	40	47204	1	1	1	1	0.09	Alpha-N-acetylgalactosaminidase OS=Mus musculus OX=10090 GN=Naga PE=1 SV=2
1468	1	SwissProt	NDUA7_MOUSE	Ndufa7	40	12568	1	1	1	1	0.39	NADH dehydrogenase [ubiquinone] 1 alpha subcomplex subunit 7 OS=Mus musculus OX=10090 GN=Ndufa7 PE=1 SV=3
196	3	SwissProt	MYO5B_MOUSE	Myo5b	39	210438	2	2	2	2	0.04	Unconventional myosin-Vb OS=Mus musculus OX=10090 GN=Myo5b PE=1 SV=2
1476	1	SwissProt	THIKA_MOUSE	Acaa1a	39	43926	2	2	2	2	0.21	3-ketoacyl-CoA thiolase A, peroxisomal OS=Mus musculus OX=10090 GN=Acaa1a PE=1 SV=1
1479	1	SwissProt	PCKGM_MOUSE	Pck2	39	70482	1	1	1	1	0.06	Phosphoenolpyruvate carboxykinase [GTP], mitochondrial OS=Mus musculus OX=10090 GN=Pck2 PE=1 SV=1
1483	1	SwissProt	DHRS1_MOUSE	Dhrs1	39	33983	2	2	2	2	0.28	Dehydrogenase/reductase SDR family member 1 OS=Mus musculus OX=10090 GN=Dhrs1 PE=1 SV=1
1484	1	SwissProt	S38AA_MOUSE	Slc38a10	39	117120	1	1	1	1	0.04	Putative sodium-coupled neutral amino acid transporter 10 OS=Mus musculus OX=10090 GN=Slc38a10 PE=1 SV=2
333	3	SwissProt	ACADL_MOUSE	Acadl	38	47877	2	2	2	2	0.19	Long-chain specific acyl-CoA dehydrogenase, mitochondrial OS=Mus musculus OX=10090 GN=Acadl PE=1 SV=2
1511	1	SwissProt	LY65B_MOUSE	Ly6g5b	38	21601	1	1	1	1	0.21	Lymphocyte antigen 6 complex locus protein G5b OS=Mus musculus OX=10090 GN=Ly6g5b PE=1 SV=1
1489	1	NCBIprot	FSIP2_MOUSE	Fsip2	38	784366	1	1	1	1	0.01	RecName: Full=Fibrous sheath-interacting protein 2
1490	1	SwissProt	MSPD2_MOUSE	Mospd2	37	59817	2	2	2	2	0.15	Motile sperm domain-containing protein 2 OS=Mus musculus OX=10090 GN=Mospd2 PE=1 SV=2

doi:10.6342/NTU201903813

1527	1	SwissProt	NDUS1_MOUSE	Ndufs1	37	79726	3	3	3	3	0.17	NADH-ubiquinone oxidoreductase 75 kDa subunit, mitochondrial OS=Mus musculus OX=10090 GN=Ndufs1 PE=1 SV=2
1544	1	SwissProt	ABCD3_MOUSE	Abcd3	36	75426	1	1	1	1	0.06	ATP-binding cassette sub-family D member 3 OS=Mus musculus OX=10090 GN=Abcd3 PE=1 SV=2
1548	1	SwissProt	RAB10_MOUSE	Rab10	36	22527	1	1	1	1	0.21	Ras-related protein Rab-10 OS=Mus musculus OX=10090 GN=Rab10 PE=1 SV=1
1560	1	SwissProt	TM9S4_MOUSE	Tm9sf4	35	74644	2	2	2	2	0.12	Transmembrane 9 superfamily member 4 OS=Mus musculus OX=10090 GN=Tm9sf4 PE=1 SV=1
1562	1	SwissProt	SCAM1_MOUSE	Scamp1	35	38004	1	1	1	1	0.12	Secretory carrier-associated membrane protein 1 OS=Mus musculus OX=10090 GN=Scamp1 PE=1 SV=1
1564	1	SwissProt	SUCA_MOUSE	Suclg1	35	36132	1	1	1	1	0.12	Succinate--CoA ligase [ADP/GDP-forming] subunit alpha, mitochondrial OS=Mus musculus OX=10090 GN=Suclg1 PE=1 SV=4

doi:10.6342/NTU201903813